

1 Measuring  $\beta$ -diversity by remote sensing: a  
2 challenge for biodiversity monitoring

3 Duccio Rocchini <sup>1,2,3,\*</sup>, Sandra Luque <sup>4</sup>, Nathalie Pettorelli <sup>5</sup>,  
Lucy Bastin <sup>6,7</sup>, Daniel Doktor <sup>8</sup>, Nicolás Faedi <sup>3,9</sup>,  
Hannes Feilhauer <sup>10</sup>, Jean-Baptiste Féret <sup>4</sup>, Giles M. Foody <sup>11</sup>,  
Yoni Gavish <sup>12</sup>, Sergio Godinho <sup>13</sup>, William E. Kunin <sup>14</sup>,  
Angela Lausch <sup>8</sup>, Pedro J. Leitão <sup>15,16</sup>, Matteo Marcantonio <sup>17</sup>,  
Markus Neteler <sup>18</sup>, Carlo Ricotta <sup>19</sup>, Sebastian Schmidlein <sup>20</sup>,  
Petteri Vihervaara<sup>21</sup>, Martin Wegmann <sup>22</sup>,  
Harini Nagendra <sup>23</sup>

4 November 1, 2017

5 <sup>1</sup> Center Agriculture Food Environment, University of Trento, Via E.  
6 Mach 1, 38010 S. Michele all'Adige (TN), Italy

7 <sup>2</sup> Centre for Integrative Biology, University of Trento, Via Sommarive,  
8 14, 38123 Povo (TN), Italy

9 <sup>3</sup> Fondazione Edmund Mach, Research and Innovation Centre, Depart-  
10 ment of Biodiversity and Molecular Ecology, Via E. Mach 1, 38010 S. Michele  
11 all'Adige (TN), Italy, corresponding author: ducciorocchini@gmail.com, duc-  
12 cio.rocchini@fmach.it

13 <sup>4</sup> UMR-TETIS, IRSTEA Montpellier, Maison de la Télédétection, 500  
14 rue JF Breton, 34093, Montpellier Cedex 5, France

15 <sup>5</sup> Institute of Zoology, The Zoological Society of London, Regent's Park,  
16 London, United Kingdom

17 <sup>6</sup> School of Computer Science, Aston University, United Kingdom

18 <sup>7</sup> Currently on secondment to Knowledge Management Unit, Joint Re-  
19 search Centre of the European Commission, Italy

20 <sup>8</sup> Helmholtz Centre for Environmental Research - UFZ, Department Com-  
21 putational Landscape Ecology Permoserstrasse 15, 04318 Leipzig, Germany

22 <sup>9</sup> Department of Computer Science and Engineering, University of Bologna,  
23 Mura Anteo Zamboni, 7, 40126 Bologna, Italy

24 <sup>10</sup> Institut für Geographie Friedrich-Alexander Universität Erlangen-Nürnberg  
25 Wetterkreuz 15, 91058 Erlangen, Germany

26 <sup>11</sup> School of Geography, University of Nottingham, Nottingham, NG7  
27 2RD, United Kingdom

28 <sup>12</sup> School of Biology, Faculty of biological Science, University of Leeds,  
29 Leeds LS2 9JT, United Kingdom

30 <sup>13</sup> Universidade de Evora , Evora · Institute of Mediterranean Agricultural  
31 and Environmental Sciences (ICAAM)

32 <sup>14</sup> School of Biology, University of Leeds, Leeds, UK

33 <sup>15</sup> Department Landscape Ecology and Environmental System Analy-  
34 sis, Technische Universität Braunschweig, Langer Kamp 19c, 38106 Braun-  
35 schweig, Germany

36 <sup>16</sup> Geography Department, Humboldt-Universität zu Berlin, Unter den  
37 Linden 6, 10099 Berlin, Germany

38 <sup>17</sup> Department of Pathology, Microbiology, and Immunology, School of  
39 Veterinary Medicine, University of California, Davis, USA

40 <sup>18</sup> Mundialis GmbH & Co. KG, Kölnstraße 99, 53111 Bonn, Germany

41 <sup>19</sup> Department of Environmental Biology, University of Rome “La Sapienza”,  
42 00185 Rome, Italy

43 <sup>20</sup> Karlsruher Institut für Technologie (KIT), Institut für Geographie und  
44 Geoökologie, Kaiserstr. 12, 76131 Karlsruhe, Germany

45 <sup>21</sup> Finnish Environment Institute (SYKE), Natural Environment Centre  
46 Mechelininkatu 34a,P.O.Box 140 FI-00251 Helsinki, Finland

47 <sup>22</sup> Department of Remote Sensing, Remote Sensing and Biodiversity Re-  
48 search Group, University of Wuerzburg, Wuerzburg, Germany

49 <sup>23</sup> Azim Premji University, PES Institute of Technology Campus, Pixel  
50 Park, B Block, Electronics City, Hosur Road, Bangalore, 560100, India

## 51 **Abstract**

52 Biodiversity includes multiscalar and multitemporal structures and  
53 processes, with different levels of functional organization, from genetic  
54 to ecosystemic levels. One of the mostly used methods to infer bio-  
55 diversity is based on taxonomic approaches and community ecology  
56 theories. However, gathering extensive data in the field is difficult due  
57 to logistic problems, [especially](#) when aiming at modelling biodiversity  
58 changes in space and time, which assumes statistically sound sampling  
59 schemes. In this [context](#), [airborne](#) or satellite remote sensing allow [in-](#)  
60 [formation to be gathered](#) over wide areas in a reasonable time.

61 Most of the biodiversity maps obtained from remote sensing have  
62 been based on the inference of species richness by regression analy-  
63 sis. On the contrary, estimating compositional turnover ( $\beta$ -diversity)

64 might add crucial information related to relative abundance of dif-  
65 ferent species instead of just richness. Presently, few studies have  
66 addressed the measurement of species compositional turnover from  
67 space.

68 Extending on previous work, in this manuscript we propose novel  
69 techniques to measure  $\beta$ -diversity from airborne or satellite remote  
70 sensing, mainly based on: i) multivariate statistical analysis, ii) the  
71 spectral species concept, iii) self-organizing feature maps, iv) multi-  
72 dimensional distance matrices, and the v) Rao's Q diversity. Each  
73 of these measures addresses one or several issues related to turnover  
74 measurement. This manuscript is the first methodological example  
75 encompassing (and enhancing) most of the available methods for es-  
76 timating  $\beta$ -diversity from remotely sensed imagery and potentially  
77 relating them to species diversity in the field.

78 *Keywords:*  $\beta$ -diversity, Kohonen self-organising feature maps, Rao's Q  
79 diversity index, remote sensing, satellite imagery, Sparse Generalized Dis-  
80 similarity Model, spectral species concept.

## 81 1 Introduction

82 Biodiversity cannot be fully investigated without considering the spatial com-  
83 ponent of its variation. In fact, it is known that the dispersal of species over  
84 wide areas is driven by spatial constraints directly related to the distance  
85 among sites. A negative exponential dispersal kernel is usually adopted to  
86 mathematically describe the occupancy of new sites by species, as:

$$F = \sum_{K=1}^N e^{\frac{-d_{ik}}{a}} \quad (1)$$

87 where  $d_{ik}$  = distance between two locations  $i$  and  $k$  and  $a$  is a parameter  
88 regulating the dispersal from localized areas (low values of  $a$ ) to widespread  
89 ones (high values of  $a$ , Meentemeyer et al. (2008)).

90 In this sense, distance acquires a significant role in ecology to estimate bio-  
91 diversity change. Hence, spatially explicit methods have been acknowledged  
92 in ecology for providing robust estimates of diversity at different hierarchical  
93 levels: from individuals (Tyre et al., 2001), to populations (Vernesi et al.,  
94 2012), to communities (Rocchini et al., 2005).

95 When dealing with spatial explicit methods, remote sensing images repre-  
96 sent a powerful tool, particularly when coupling information on compositional  
97 properties of the landscape with its structure (Figure 1). Remote sensing has

98 widely been used for conservation practices including very different types of  
99 data such as nightlights data (Mazor et al., 2013), Land Surface Temperature  
100 estimated from MODIS data (Metz et al., 2014), spectral indices (Gillespie,  
101 2005).

102 Most of the remote sensing applications for biodiversity estimation have  
103 relied on the estimate of local diversity hotspots, considering land use diver-  
104 sity (Wegmann et al., 2017) or continuous spatial variability of the spectral  
105 signal (Rocchini et al., 2010). This is mainly grounded in the assumption  
106 that a higher landscape heterogeneity is strictly related to a higher amount  
107 of species occupying different niches. However, given two sites  $s_1$  and  $s_2$ , the  
108 final diversity is not only related to the species / spectral richness of  $s_1$  and  
109  $s_2$ , but overall to the amount of shared species / spectral values. In other  
110 words, the lower the their intersection  $s_1 \cap s_2$ , the higher will be the total  
111 diversity, while a low total diversity will be reached when  $s_1 \cap s_2 = s_1 \cup s_2$ .  
112 Such intersection has been widely studied in ecology, after the development  
113 of  $\beta$ -diversity theory (Whittaker, 1960).

114 Tuomisto et al. (2003) demonstrated the power of substituting distance in  
115 Eq. 1 by spectral distance to directly account for the distance between sites  
116 in an environmental space, instead of a merely spatial one. However, while  
117 spectral distance examples exist when measuring the  $\beta$ -diversity among pairs  
118 of sites (e.g. Rocchini et al. (2015)), few studies have tested the possibility of  
119 measuring  $\beta$ -diversity over wide areas considering several sites at the same  
120 time (however see Alahuhta et al. (2017); Harris et al. (2015)). This is  
121 especially true when considering the development of remote sensing tools  
122 for diversity estimate in which the concept of  $\beta$ -diversity is still pioneering.

123 The aim of this paper is to present the most novel methods to measure  
124  $\beta$ -diversity from remotely sensed imagery based on the the most recently  
125 published ecological models. In particular we will deal with: i) multivariate  
126 statistical techniques, ii) the applicability of the spectral species concept,  
127 iii) multidimensional distance matrices, iv) metrics coupling abundance and  
128 distance-based measures.

129 This manuscript is the first methodological example encompassing (and  
130 enhancing) most of the available methods for estimating  $\beta$ -diversity from  
131 remotely sensed imagery and potentially relate them to species diversity in  
132 the field.

## 133 2 Multivariate statistical analysis for species 134 diversity estimate from remote sensing

135 Univariate statistics have been used to directly find relations between spectral  
136 and species diversity. However, the amount of variability explained by single  
137 bands / vegetation indices versus species diversity is generally relatively low,  
138 due to the fact that different aspects related to the complexity of habitats  
139 might act in shaping diversity, from disturbance and land use at local scales  
140 to climate and element fluxes at global scales.

141 Ordination techniques are designed to quantitatively describe multivari-  
142 ate gradual transitions in the species composition of sampled sites. Measuring  
143 the distance between two sampling sites in the multi-dimensional ordination  
144 space is a good proxy of the change in species composition. When this mea-  
145 sure is related to the geographical distance between the considered sites, the  
146 beta diversity at this particular scale can be assessed.

147 Of the various available ordination techniques, Detrended Correspon-  
148 dence Analysis (DCA, Hill and Gauch (1980)) is particularly suitable for  
149 such analyses. The axes (i.e. gradients) of the DCA ordination space are  
150 scaled in standard deviation (SD) units, where a distance of 4 SD is related  
151 to a full species turnover. This enables a versatile analysis that easily reveals  
152 whether two sampled sites still have species in common.

153 Several studies have mapped the ordination space using remote sensing  
154 data (e.g., Schmidtlein and Sassini (2004); Schmidtlein et al. (2007); Feil-  
155 hauer et al. (2009, 2011, 2014); Gu et al. (2015); Harris et al. (2015); Leitao  
156 et al. (2015); Neumann et al. (2015)). For this purpose, the axes scores of  
157 the sampled sites are regressed against the corresponding canopy reflectance  
158 values extracted from air- or spaceborne image data. The resulting multi-  
159 variate regression models, one per ordination axis and most often generated  
160 with machine learning regression techniques, are subsequently applied on the  
161 image data for a spatial prediction of ordination scores. Each pixel of the  
162 image data is assigned to a specific position in the ordination space that in-  
163 dicates its species composition. The resulting gradient maps are a powerful  
164 tool for analyses of beta diversity across different spatial scales (Feilhauer et  
165 al., 2009; Hernandez-Stefanoni et al., 2012).

166 A simple analysis of the variability of the DCA scores in a defined pixel  
167 neighborhood (i.e. a moving window) results in a efficient beta diversity  
168 assessment. The spatial scale of this assessment can be varied either by  
169 re-sampling the gradient map to a coarser spatial resolution (i.e. pixel size) or  
170 by changing the kernel size of the considered pixel neighborhood. Such tech-  
171 niques have been further developed e.g. for spatial conservation prioritization

172 programmes such as [Zonation](#) (Moilanen et al., 2005, 2009).

173 Figure 2 shows an example of a DCA-based assessment of beta diversity  
174 on a very local scale (10 m) following the approach described in Feilhauer et  
175 al. (2009). The analyzed landscape is a mosaic of raised bogs, fens, transition  
176 mires and *Molinia* meadows. For a detailed description of the data and site  
177 please refer to Feilhauer et al. (2014, 2016).

178 Analyses like this require two different data sets: (1) a sample of field  
179 data that is representative for the vegetation in the studied area and is used  
180 to generate the ordination space; (2) image data with a sufficient spectral  
181 resolution to discriminate the vegetation types within the ordination space  
182 and with a spatial resolution that is in line with the sampling design of the  
183 field data (Feilhauer et al., 2013).

184 Using these data, the continuous spatial variability of the spectral signal  
185 in the image pixels is translated into a spatially continuous measure of species  
186 composition. The advantages of this approach are obvious: since the diversity  
187 analyses are conducted in the floristic gradient space, the resulting measures  
188 resemble field studies and are thus easier to interpret than spectral proxies  
189 and closer to the point of view of many end-users. [Furthermore](#), the analysis  
190 of ordination scores in defined pixel neighborhoods is not restricted to a  
191 single spatial scale but offers the opportunity to implement assessments of  
192 beta diversity on multiple scales.

### 193 **3 The spectral species concept**

194 The spectral species concept has been proposed by Féret and Asner (2014a)  
195 to map both  $\alpha$  and  $\beta$  component of the biodiversity using a unique frame-  
196 work. It is rooted in the convergence between two other concepts, the spec-  
197 tral variation hypothesis (SVH) proposed by Palmer et al. (2002), and the  
198 plant optical types proposed by Ustin and Gamon (2010), sustained by the  
199 technological advances in the domain of high spatial resolution imaging spec-  
200 troscopy. The SVH states that the spatial variability in the remotely sensed  
201 signal, that is the spectral heterogeneity, is related to environmental hetero-  
202 geneity and could therefore be used as a powerful proxy of species diversity.  
203 SVH has been tested in different situations (Rocchini et al., 2010) and con-  
204 clusions show that the [performance](#) of this approach is very dependent on  
205 several factors, including the [instrument](#) characteristics (spectral, spatial and  
206 temporal resolution), the type of vegetation investigated, and the metrics de-  
207 rived from remotely sensed information to estimate spectral heterogeneity.  
208 Plant optical types refer to the capacity of sensors to measure [signals that](#)  
209 [aggregate](#) information about vegetation structure, phenology, biochemistry

210 and physiology. Therefore, this concept is also tightly linked to the perfor-  
211 mances of the sensor and finds particular echo with the increasing use of high  
212 spatial resolution imaging spectroscopy for the estimation and identification  
213 of multiple vegetations properties.

214 The details provided by high spatial resolution imaging spectroscopy are  
215 sufficient to perform analyses of plant optical traits at the individual tree scale  
216 in order to differentiate tree species, obtain information about leaf chemical  
217 traits and estimate the  $\alpha$  component of biodiversity (Asner et al., 2008, 2015;  
218 Chadwick and Asner, 2016; Clark et al., 2005; Clark and Roberts, 2012;  
219 Féret and Asner, 2013; Vaglio Laurin et al., 2014). These results illustrate  
220 that spectral information can be related to taxonomic or functional informa-  
221 tion of the vegetation, which supports the SVH under the hypothesis that  
222 the metrics used to compute spectral heterogeneity and a given component  
223 of vegetation diversity are properly defined. However these applications are  
224 currently limited by the important amount of field data required to train re-  
225 gression or classification models, which is also directly linked to their low gen-  
226 eralization ability in time and space. Unsupervised approaches then appear  
227 as valuable alternatives for the analysis of ecosystem heterogeneity (Baldeck  
228 and Asner, 2013; Baldeck et al., 2014; Feilhauer et al., 2011; Baldeck and  
229 Asner, 2013; Féret and Asner, 2014b), as ecological indicators of  $\alpha$  and  $\beta$   
230 diversity at landscape scale usually require one or several levels of abstraction  
231 beyond the correct taxonomic identification (Tuomisto et al., 2006).

232 Clustering (properly pre-processed) spectral information should result in  
233 pixels from the same species naturally grouping together rather than dis-  
234 tributing randomly among clusters, Féret and Asner (2014a) proposed a  
235 grouping method aiming at assigning labels to pixels based on multiple clus-  
236 tering of spectroscopic data acquired at landscape scale. These pixels, labeled  
237 with a set of so-called spectral species, can then be used straightforwardly  
238 in order to compute various diversity metrics such as Shannon index for  $\alpha$   
239 diversity, and Bray-Curtis dissimilarity for  $\beta$  diversity. The pre-processing  
240 stage is divided into several stages. After masking all non-vegetated pixels, a  
241 normalization based on **continuous** removal is applied to each pixel and over  
242 the full spectral domain, then a principal component analysis is performed on  
243 the **continuously** removed spectral data. The normalization **reduces** effects  
244 due to changes in illumination, canopy geometry and other factors unrelated  
245 to vegetation, while enhancing the signal corresponding to vegetation. The  
246 components including individual-specific information are the components of  
247 interest. They can be identified after visual inspection or automated routines,  
248 if initial data show sufficient signal to noise ratio. Once a limited number  
249 of components have been selected, k-means clustering is then applied to a  
250 certain number of subsets, and for each of these subsets, centroids are com-



251 puted and each pixel in the image is labeled based on the closest centroid.  
252 The repetition of clustering based on various subsets of the image tends to  
253 minimize the risk of assigning centroids to irrelevant groups of pixels. Ex-  
254 perimental results showed that the averaging of diversity indices computed  
255 from multiple centroid maps can be seen as an analogous to signal averaging,  
256 which consists in increasing signal to noise ratio by replicating measurements.  
257 For each repetition, the closest centroid corresponds to the spectral species,  
258 and for each spatial unit of a given size, the spectral species distribution is  
259 derived in order to compute any diversity metric requiring either information  
260 at the local scale, or comparison of information across spatially distant plots.

261 The concepts of spectral species and spectral species distribution have  
262 been tested successfully on a limited number of situations and types of  
263 ecosystems (see (Rocchini et al., 2016) for a review, and (Lausch et al.,  
264 2016) for an application to similar concepts). As an example, F eret and  
265 Asner (2014a) showed ability to properly estimate landscape heterogeneity  
266 at moderate spatial scale, up to few dozen square kilometers over tropical  
267 forests, based on high spatial resolution imaging spectroscopy (Figure 3).  
268 A generic parameterization of the method showed robust performances for  
269  $\alpha$  diversity mapping across space and time, but mapping  $\beta$  diversity across  
270 large spatial scales using images acquired during different airborne campaign  
271 remains challenging, which leads to an unsolved problem when considering  
272 operational regional mapping. In the perspective of global monitoring of  
273 biodiversity, and given the unprecedented remote sensing capacity allowed  
274 by the Copernicus program, including the Sentinel-2 multispectral satellites,  
275 several other challenges are foreseen and currently investigated. The influ-  
276 ence of decreased spatial and spectral resolution on the ability to properly  
277 differentiate ecologically meaningful spectral species across landscapes and  
278 over regions will need to be investigated. The application of this concept be-  
279 yond tropical forests and savanna ecosystems should also be investigated, as  
280 it may not hold when applied on moderately diverse ecosystems or systems  
281 with individuals whose individuals have dimensions well below the resolving  
282 power of the instrument.

## 283 4 Self organizing feature maps

284 The Kohonen self-organising feature map (SOFM, Kohonen (1982)) is a neu-  
285 ral network that may be used to undertake unsupervised clustering of data.  
286 Critically, the input to a SOFM can be a large multi-variate data set such  
287 as may be acquired on species from quadrat based field surveys. The SOFM  
288 summarises the data in a low, typically two, dimensional output (Figure



289 4). In this output space the data for individual quadrats are topologically  
290 ordered – with sites that are similar close together while those of highly dif-  
291 ferent species composition are more distant. Because the data sites in the  
292 output space are arranged by relative similarity the output space may also  
293 be used to aggregate or classify a data set. As such the SOFM is attrac-  
294 tive as a non-parametric clustering analysis and as a means to undertake an  
295 ordination (Chon et al., 1996).

296 A SOFM is, unlike some of the approaches used commonly in community  
297 ecology, not constrained by assumptions relating the statistical distribution  
298 of the data used. The SOFM uses unsupervised learning to produce a topo-  
299 logically ordered output space in which the samples are arranged spatially  
300 in relation to their relative similarity in species composition. The SOFM  
301 thus performs a non-parametric ordination analysis (Foody, 1999). The pro-  
302 duction of a classification by a SOFM comprises two main stages (Giraudel  
303 and Lek, 2001). An iterative analysis, in which time-decaying parameters  
304 that control network learning and the size of local neighbourhoods located  
305 around output units, is used. For this, the user must specify a number of key  
306 parameters such as the size and shape of the network, number of iterations of  
307 the algorithm, the learning rate and its rate of decline and a neighbourhood  
308 parameter. The need for such parameters can add some uncertainty to the  
309 analysis. While there are no formal rules to follow in the design of a SOFM  
310 there are recommendations for the determination of SOFM parameter set-  
311 tings (Giraudel and Lek, 2001). A further concern is that as an unsupervised  
312 classifier the classes defined may not always be the most useful for an in-  
313 vestigation. In addition, the nature of the analysis means the direction of  
314 the gradients cannot be controlled (Fritzke, 1995) but the analysis performs  
315 well in comparison to popular ordination techniques such as PCA and DCA  
316 (Foody and Cutler, 2003). The SOFM may also use a variety of different  
317 data types such as presence/absence, abundance or importance values and  
318 can solve complex non-linear problems (Giraudel and Lek, 2001).

## 319 5 Multidimensional distance matrices: GDMs 320 and SGDMs

321 One of the most widespread methods for assessing  $\alpha$ -diversity is using distance  
322 matrices (Legendre et al., 2005). Indeed, early work by Whittaker (1960) sug-  
323 gested that  $\beta$ -diversity could be quantified by dissimilarity matrices among  
324 (pairs of) sites. Furthermore, the Mantel test (Mantel and Valand, 2017),  
325 designed to estimate the association between two independent dissimilarity

326 matrices, has been widely used to correlate a community composition dissim-  
327 ilarity matrix with an environment dissimilarity one, thus providing useful  
328 insights into community composition and turnover (Legendre et al., 2005;  
329 Tahvanainen et al., 2011).

330 Generalized Dissimilarity Modelling (GDM; Ferrier (2007) can be con-  
331 sidered as an extension of the Mantel test, which is able to accommodate  
332 multidimensional environmental data, to be compared with the composi-  
333 tional data. GDMs also allow for the prediction of compositional turnover  
334 as well as for, e.g. environmental classification constrained to the compo-  
335 sitional dissimilarity (Ferrier, 2007; Leathwick et al., 2011). In GDM, the  
336 compositional dissimilarities between all pairs of samples are modelled as a  
337 function of their respective environmental distances. This is done through a  
338 linear combination of monotonic I-spline basis functions, under the assump-  
339 tion that increasing environmental dissimilarity (e.g. along a gradient) can  
340 only result in increasing compositional dissimilarity. This method is thus well  
341 suited for measuring and mapping  $\beta$ -diversity, and is thus becoming widely  
342 used in conservation science and macroecology, and recently been subject to  
343 several developments as we describe below.

344 One such development is the phylogenetic GDM (phylo-GDM; Rosauer  
345 et al. (2014)), which incorporates phylogenetic dissimilarities into GDM and  
346 allows for analysing and predicting phylogenetic  $\beta$ -diversity, thus linking  
347 ecological and evolutionary processes. This method can provide novel in-  
348 sights into the mechanisms underlying current patterns of biological diversity  
349 (Graham et al., 2008). Another recent development of GDM is the multi-  
350 site GDM (MS-GDM; Latombe et al. (2017)), which extends GDMs from  
351 pairwise to multi-site dissimilarity modelling. In such paper, the authors  
352 tested MS-GDM by means of both constrained (monotonical) additive mod-  
353 els and I-splines, although with no conclusive results relating to the best  
354 method overall. They concluded, however, that when applying MS-GDM to  
355 a high number of samples, they could better explain the drivers of species  
356 turnover. Also, an important development of GDM is the Bayesian bootstrap  
357 GDM (BBGDM; Woolley et al. (2017)) designed to characterize uncertainty  
358 in generalized dissimilarity models. This approach allows better represent-  
359 ing the underlying uncertainty in the data, by estimating the variance in  
360 parameters based on the available data.

361 Finally, an implementation of GDM, which was created particularly for  
362 dealing with high-dimensional (and potentially high-collinear) remote sensing  
363 data as input in GDM is the Sparse Generalized Dissimilarity Model (SGDM,  
364 Figure 5, Leitao et al. (2015)). This method is a two-stage approach that  
365 consists of initially reducing the environmental space (e.g. reflectance data)  
366 by means of a Sparse Canonical Correlation Analysis (SCCA, Figure 5; Wit-

367 ten et al. (2013)), and then fitting the resulting components with a GDM  
 368 model. The SCCA is a form of penalized canonical correlation analysis based  
 369 on the L1 (lasso) penalty function, and is thus designed to deal with high-  
 370 dimensional data. The two algorithms are coupled in a way that the SCCA  
 371 penalization is selected through a heuristic grid search manner, in order to  
 372 minimize the cross-validate root mean square error in the dissimilarities pre-  
 373 dicted by the GDM. In this procedure, the high-dimensional environmental  
 374 data (such as coming from time series of multispectral or hyperspectral data)  
 375 are subject to a supervised ordination approach that reduces their dimen-  
 376 sion while capturing the axes of variation that most correlate to those of  
 377 the community compositional matrix. SGDM has been successfully used for  
 378 modelling and mapping the compositional turnover of both animal and plant  
 379 species, using several different sources of remote sensing (and auxiliary) data  
 380 (Leitao et al., 2015; Leitão et al., 2017).

## 381 6 Rao's Q diversity

382 Most of the previously shown metrics are based on the distance among pixel  
 383 values in a multidimensional spectral space. None of them considers the  
 384 relative abundance of such pixel values in a neighbourhood.

385 By contrast, abundance-based metrics such as the Shannon entropy could  
 386 output similar results despite a variable distance among pixel values. As an  
 387 example, consider a 3x3 matrix of remotely sensed data:

$$\begin{pmatrix} x_{11} & x_{12} & x_{13} \\ x_{21} & x_{22} & x_{23} \\ x_{d1} & x_{d2} & x_{d3} \end{pmatrix} \quad (2)$$

388 composed by the following values:

$$\begin{pmatrix} 10 & 13 & 15 \\ 18 & 20 & 23 \\ 19 & 21 & 22 \end{pmatrix} \quad (3)$$

389 then consider a different matrix:

$$\begin{pmatrix} 10 & 121 & 227 \\ 1 & 40 & 251 \\ 7 & 100 & 149 \end{pmatrix} \quad (4)$$

390 From a Shannon's entropy perspective, such matrices are equal in terms of  
 391 heterogeneity. The Shannon's entropy is indeed based on the relative abun-  
 392 dance (and richness) of a sample, and its value is 2.197 for both the matrices.

393 This value, equalling the natural logarithm of the number of classes (pixel  
394 values), is also Shannon's maximum theoretical value given a 3x3 matrix,  
395 due to the lack of identical numbers in the matrices. This example explicitly  
396 shows that accounting for the distance among values and their relative abun-  
397 dance is crucial to discriminate among areas in terms of measured (modeled)  
398 heterogeneity.

399 One of the metrics accounting for both the abundance and the pairwise  
400 spectral distance among pixels is the Rao's Q diversity index, as:

$$Q = \sum \sum d_{ij} \times p_i \times p_j \quad (5)$$

401 where  $d_{ij}$  = spectral distance among pixels  $i$  and  $j$  and  $p$  = proportion of  
402 occupied area.

403 Hence, Rao's Q is capable of discriminating among the ecological diversity  
404 of matrices 3 and 4, turning out to be 4.59 and 90.70, respectively. Appendix  
405 1 provide an example spreadsheet to perform the calculation while the com-  
406 plete R code is stored in the GitHub repository  
407 <https://github.com/mattmar/spectralrao>.

408 We decided to make use of a case study to highlight the importance of  
409 considering the distance among pixel values in remote sense ecological appli-  
410 cation. The performance of Rao's Q index in describing landscape diversity  
411 was tested in a complex agro-forestry landscape located in southern Portu-  
412 gal. A test site with an area of about  $10 \times 10 \text{ km}^2$  (centroid located at  $38^\circ$   
413  $39' 10.74''$  N;  $8^\circ 12' 52.30''$  W) was selected to conduct the analysis. In this  
414 area, a savanna-like ecosystem called montado occupies about 40% of the test  
415 site, followed by traditional olive groves, pastures, vineyards, and irrigated  
416 monocultures (e.g. corn fields). Montado is spatially characterized by the  
417 variability of its tree density (e.g. Godinho et al. (2016)), and the gradient  
418 between low and high tree density over space can lead to different structural  
419 heterogeneity and habitat diversity.

420 Within the test site, polyculture under small farming context (e.g. veg-  
421 etable gardens, orchards, and cereal crops) is an important feature of this  
422 landscape by generating a high compositional and configurational spatial  
423 heterogeneity (Figure 6). The main goal in using this case study is to demon-  
424 strate the potential and effectiveness of the Rao's Q index in producing ac-  
425 curately remote-sensing based maps of spatial diversity over such complex  
426 landscape. For this study, a cloud-free Sentinel-2A (S2A) image acquired  
427 on 8 of August 2016 was used to compute the NDVI at a 10 meters spatial  
428 resolution. The S2A image download, as well as the atmospheric correction  
429 (DOS method) were performed using the Semi-Automatic Classification plu-  
430 gin (SCP) implemented in the QGIS software (QGIS Development Team ,  
431 2016(@)).

432 The NDVI was used as input data for Rao's Q index computation using  
433 a window size of  $3 \times 3$  pixels. The performance of the Rao's Q was compared  
434 to the Shannon Entropy index (Shannon's H), which is one of the simplest,  
435 and widely used, remote sensing-based diversity measures for landscape het-  
436 erogeneity assessment (Rocchini et al., 2016). To investigate whether both  
437 diversity indices differ between land cover types, one-way ANOVA tests were  
438 performed. This approach was used for analysing the degree of dissimilarity  
439 between Rao's Q and Shannon H index across two high complex land cover  
440 types; i) montado, and ii) polyculture. To do so, a sample of 60 squares with  
441  $250 \times 250$  meters size was randomly selected over these two land cover types.  
442 Each square represents a sample of 625 S2A NDVI pixels, thus corresponding  
443 to a total of 37,500 pixels over the 60 squares. For the comparison between  
444 both indices, the coefficient of variation (CV) was calculated for each  $250 \times$   
445  $250$  m squares. Regarding the Rao's Q performance, Figure 6 clearly points  
446 to the significant improvements shown by Rao's Q index compared to the  
447 Shannon H index in describing the spatial diversity. In particular, it can be  
448 seen through the Figure 6, that Rao's Q index can highlight different gra-  
449 dients of spatial diversity of montado areas, which present high tree density  
450 variability (Figure 6), and thus high spatial heterogeneity. One-way ANOVA  
451 tests revealed that both indices values were significantly different between  
452 the two land cover types (montado:  $F = 503.3$ ,  $p < 0.001$ ; polyculture:  $F =$   
453  $889.8$ ,  $p < 0.001$ ). Overall, the obtained results demonstrate the capability of  
454 Rao's Q index in producing accurate landscape diversity maps in a complex  
455 landscape such as the Mediterranean agro-forestry systems.

## 456 7 Conclusion

457 In this paper, we showed several methods based on ecological  $\beta$ -diversity,  
458 which can be investigated by remote sensing through the calculation of  
459 ecosystem heterogeneity, to estimate the spatial variability of biodiversity.  
460 When there is a wide range of heterogeneity, for example when the data  
461 include homogeneous and heterogeneous zones, no single measure might cap-  
462 ture all the different aspects of  $\beta$ -diversity (e.g. Baselga (2013)). That is why  
463 we suggested in this manuscript multivariate and multidimensional methods  
464 (e.g. multivariate statistics and multidimensional distance matrices) based  
465 on the spectral signal and its variability over space to account for different  
466 aspects of diversity, also including distance- and abundance-based methods  
467 (e.g. the Rao's Q).

468 Biodiversity measured as species richness is often used for conservation  
469 purposes, hence the importance of avoiding an under- or over-estimate has

470 been highlighted (Chiarucci et al., 2009). Furthermore, pairwise distance-  
 471 based methods might be profitably used to detect not only diversity hotspots  
 472 in an area but also the variation of biodiversity over space, and potentially  
 473 over time, once multitemporal sets of images are used.

474 In this paper we focused on optimising measures of  $\beta$ -diversity based on  
 475 remote sensing data. Such measures might be used to regress species diversity  
 476 against remotely sensed heterogeneity, based on new regression techniques  
 477 which maximise the possibility of predicting the zones in a study area, or at  
 478 larger spatial scales, of peculiar conservation value. As an example, shrink-  
 479 age regression, recently applied in biodiversity conservation (Authier et al.,  
 480 2017) could allow a direct focus on habitat modelling, which is one of the  
 481 major strengths of remote sensing (Gillespie et al., 2008). Moreover, such  
 482 analysis might be performed in a Bayesian framework allowing to i) model  
 483 multidimensional covariates with non-stationary variation over space (Ran-  
 484 dell et al., 2016), such as the bands of satellite images, and ii) model the  
 485 errors in the output and their variation over space (Rocchini et al., 2017).

486 As previously stated, the suggested methods for  $\beta$ -diversity estimation  
 487 from remote sensing are mainly based on distances, but they could be effec-  
 488 tively translated to relative abundance-based methods. As an example Roc-  
 489 chini et al. (2013) introduced the possibility of applying generalized entropy  
 490 theory to satellite images with one single formula representing a continuum  
 491 of diversity measures changing one parameter. One of the best examples  
 492 in this framework could be the use of Hill numbers, in which diversity is  
 493 expressed as:

$${}^qD = \left( \sum_{i=1}^S p_i^q \right)^{\frac{1}{1-q}} \quad (6)$$

494 where  $S$  = number of samples / pixels and  $p_i$  = relative abundance of a  
 495 species / spectral value. varying the parameter  $q$ ,  ${}^qD$  varies accordingly in  
 496 several diversity indices, e.g. for  $q = 0$   ${}^qD$  is the simple number of species,  
 497 for  $\lim(q) = 1$   ${}^qD$  equals Shannon's entropy, etc. (Hsieh et al., 2016).

498 Furthermore, connectivity analysis might also be taken into account (Moila-  
 499 nen et al., 2005, 2009). For instance, a remote sensing based connectivity  
 500 network among different sites, based on  $\beta$ -diversity measures, could be ap-  
 501 plied for the estimate of landscape connectivity and consequent genetic flow,  
 502 as demonstrated by Vernesi et al. (2012). It has also been shown that commu-  
 503 nity related biodiversity indicators are often missing from current monitoring  
 504 programmes (Vihervaara et al., 2017); thus methods such as remote sensing  
 505 based Rao's Q diversity applied for various ecosystems might improve other-  
 506 wise challenging monitoring of biological communities.

507 With this manuscript we hope to stimulate discussion on the available  
508 methods for estimating  $\beta$ -diversity from remotely sensed imagery by propos-  
509 ing innovative techniques grounded on ecological theory.

## 510 Acknowledgments

511 We are grateful to the handling Editor and to two anonymous reviewers  
512 who improved with skillful suggestions a previous version of the present  
513 manuscript.

## 514 Authors' contribution statement

515 All authors contributed to the development and writing of the manuscript.

## 516 References

- 517 Alahuhta, J., Kosten, S., Akasaka, M., Auderset, D., Azzella, M., Bolpagni,  
518 R., Bove, C.P., Chambers, P.A., Chappuis, E., Ilg, C., Clayton, J., de  
519 Winston, M., Ecke, F., Gacia, E., Gecheva, G., Grillas, P., Hauxwell,  
520 J., Hellsten, H., Hjort, J., Hoyer, M.V., Kolada, K., Kuoppala, M., Lau-  
521 ridsen, T., Li, E.-H., Lukács, B.A., Mjelde, M., Mikulyuk, A., Mormul,  
522 R.P., Nishihiro, J., Oertli, B., Rhazi, L., Rhazi, M., Sass, L., Schranz, C.,  
523 Søndergaard, M., Yamanouchi, T., Yu, Q., Wang, H., Willby, N., Zhang,  
524 X.-K., Heino, J. (2017). Global variation in the beta diversity of lake  
525 macrophytes is driven by environmental heterogeneity rather than lati-  
526 tude. *Journal of Biogeography*, in press.
- 527 Asner, G., Martin, R., 2008. Spectral and chemical analysis of tropical forests:  
528 Scaling from leaf to canopy levels. *Remote Sens. Environ.* 112, 3958–3970.  
529 doi:10.1016/j.rse.2008.07.003
- 530 Asner, G.P., Martin, R.E., Anderson, C.B., Knapp, D.E., 2015. Quantifying  
531 forest canopy traits: Imaging spectroscopy versus field survey. *Remote*  
532 *Sens. Environ.* 158, 15–27. doi:10.1016/j.rse.2014.11.011
- 533 Authier, M., Saraux, C., Peron, C. (2017). Variable selection and accurate  
534 predictions in habitat modelling: a shrinkage approach. *Ecography*, 40:  
535 549-560.



- 536 Baselga, A. (2013). Multiple site dissimilarity quantifies compositional het-  
537 erogeneity among several sites, while average pairwise dissimilarity may be  
538 misleading. *Ecography*, 36: 124-128.
- 539 Baldeck, C., Asner, G., 2013. Estimating Vegetation Beta Diversity from Air-  
540 borne Imaging Spectroscopy and Unsupervised Clustering. *Remote Sens.*  
541 5, 2057–2071. doi:10.3390/rs5052057
- 542 Baldeck, C.A., Colgan, M.S., Féret, J.-B., Levick, S.R., Martin, R.E., Asner,  
543 G.P., 2014. Landscape-scale variation in plant community composition of  
544 an African savanna from airborne species mapping. *Ecol. Appl.* 24, 84–93.  
545 doi:10.1890/13-0307.1
- 546 Chadwick, K., Asner, G., 2016. Organismic-Scale Remote Sensing of  
547 Canopy Foliar Traits in Lowland Tropical Forests. *Remote Sens.* 8, 87.  
548 doi:10.3390/rs8020087
- 549 Chiarucci, A., Bacaro, G., Rocchini, D., Ricotta, C., Palmer, M.W., Scheiner,  
550 S.M. (2009). Spatially constrained rarefaction: incorporating the autocor-  
551 related structure of biological communities in sample-based rarefaction.  
552 *Community Ecology*, 10: 209-214.
- 553 Chon, T.-S., Park, Y.S., Moon, K.Y., Cha, E.Y. (1996). Patternizing com-  
554 munities by using an artificial neural network. *Ecological Modelling*, 90:  
555 69-78.
- 556 Clark, M., Roberts, D., Clark, D., 2005. Hyperspectral discrimination of trop-  
557 ical rain forest tree species at leaf to crown scales. *Remote Sens. Environ.*  
558 96, 375–398. doi:10.1016/j.rse.2005.03.009
- 559 Clark, M.L., Roberts, D.A., 2012. Species-Level Differences in Hyperspectral  
560 Metrics among Tropical Rainforest Trees as Determined by a Tree-Based  
561 Classifier. *Remote Sens.* 4, 1820–1855. doi:10.3390/rs4061820
- 562 Feilhauer, H., Faude, U., Schmidtlein, S., 2011. Combining Isomap ordina-  
563 tion and imaging spectroscopy to map continuous floristic gradients in a  
564 heterogeneous landscape. *Remote Sens. Environ.* 115, 2513–2524.
- 565 Feilhauer, H., Doktor, D., Lausch, A., Schmidtlein, S., Schulz, G., Stenzel,  
566 S., 2014. Mapping Natura 2000 habitats and their local variability with  
567 remote sensing. *Appl. Veg. Sci.* 17, 765–779.
- 568 Feilhauer, H., Doktor, D., Schmidtlein, S., Skidmore, A.K., 2016. Mapping  
569 pollination types with remote sensing. *J. Veg. Sci.* 27, 999-1011.

- 570 Feilhauer, H., Schmidtlein, S., 2009. Mapping continuous fields of alpha and  
571 beta diversity. *Appl. Veg. Sci.* 12, 429–439.
- 572 Feilhauer, H., Thonfeld, F., Faude, U., et al., 2013. Assessing floristic com-  
573 position with multispectral sensors a comparison based on monotempo-  
574 ral and multiseasonal field spectra. *Int. J. Appl. Earth Obs. Geoinf.* 21,  
575 218–229.
- 576 Féret, J.-B., Asner, G.P., 2014a. Mapping tropical forest canopy diver-  
577 sity using high-fidelity imaging spectroscopy. *Ecol. Appl.* 24, 1289–1296.  
578 doi:10.1890/13-1824.1
- 579 Féret, J.-B., Asner, G.P., 2014b. Microtopographic controls on lowland  
580 Amazonian canopy diversity from imaging spectroscopy. *Ecol. Appl.* 24,  
581 1297–1310. doi:10.1890/13-1896.1
- 582 Féret, J.-B., Asner, G.P., 2013. Tree Species Discrimination in Tropical  
583 Forests Using Airborne Imaging Spectroscopy. *IEEE Trans. Geosci. Re-  
584 mote Sens.* 51, 73–84. doi:10.1109/TGRS.2012.2199323
- 585 Ferrier, S., Manion, G., Elith, J., Richardson, K. (2007) Using generalized  
586 dissimilarity modelling to analyse and predict patterns of beta diversity in  
587 regional biodiversity assessment. *Diversity and Distributions*, 13, 252-264.
- 588 Foody, G.M. (1999). Applications of the self-organising feature map neural  
589 network in community data analysis. *Ecological Modelling*, 120: 97-107.
- 590 Foody, G.M., Cutler, M.E.J. (2003). Tree biodiversity in protected and logged  
591 Bornean tropical rain forests and its measurement by satellite remote sens-  
592 ing. *Journal of Biogeography*, 30: 1053-1066.
- 593 Fritzke, B., 1995. Growing grid-a self organizing network with constant neigh-  
594 borhood range and adaptation strength. *Neural Processing Letters*, 2: 9-  
595 13.
- 596 Giraudel, J.L., Lek, S. (2001). A comparison of SOM algorithm and some con-  
597 ventional statistical methods for ecological community ordination. *Ecolog-  
598 ical Modelling*, 146: 329-339.
- 599 Godinho, S., Gil, A., Guiomar, N., Neves, N. and Pinto-Correia, T. 2016.  
600 A remote sensing-based approach to estimating montado canopy density  
601 using the FCD model: a contribution to identifying HNV farmlands in  
602 southern Portugal. *Agroforestry Systems* 90:23-34.

- 603 Gillespie, T.W. (2005). Predicting woody-plant species richness in tropical  
604 dry forests: a case study from South Florida, U.S.A. *Ecological Applica-*  
605 *tions*, 15: 27-37.
- 606 Gillespie, T.W., Foody, G.M., Rocchini, D., Giorgi, A.P., Saatchi, S. (2008).  
607 Measuring and modeling biodiversity from space. *Progress in Physical Ge-*  
608 *ography*, 32: 203-221.
- 609 Graham, C.H., Fine, P.V.A. (2008) Phylogenetic beta diversity: linking eco-  
610 logical and evolutionary processes across space in time. *Ecology Letters*,  
611 11, 1265-1277
- 612 Gu, H., Singh, A., Townsend, P.A., 2015. Detection of gradients of forest  
613 composition in an urban area using imaging spectroscopy. *Remote Sens.*  
614 *Environ.* 167, 168-180.
- 615 Harris, A., Charnock, R., Lucas, R.M., 2015. Hyperspectral remote sensing  
616 of peatland floristic gradients. *Remote Sens. Environ.* 162, 99–111.
- 617 Heino, J., Melo, A.S., Bini, L.M., Altermatt, F., Al-Shami, S.A, Angeler, D.,  
618 Bonada, N., Brand, C., Callisto, M., Cottenie, K., Dangles, O., Dudgeon,  
619 D., Encalada, A., Göthe, E., Grönroos, M., Hamada, N., Jacobsen, D.,  
620 Landeiro, V.L., Ligeiro, R., Martins, R.T., Miserendino, M. L., Md Rawi,  
621 C.S. Rodrigues, M., Roque, F.O., Sandin, L., Schmera, D., Sgarbi, L.F.,  
622 Simaika, J., Siqueira, T., Thompson, R.M., Townsend, C.R. (2015) A  
623 comparative analysis reveals weak relationships between ecological factors  
624 and beta diversity of stream insect metacommunities at two spatial levels.  
625 *Ecology and Evolution* 5, 1235-1248.
- 626 Hsieh, T.C., Ma, K.H., Chao, A. (2016). iNEXT: an R package for rarefaction  
627 and extrapolation of species diversity (Hill numbers). *Methods in Ecology*  
628 *& Evolution* 2016, 7: 1451-1456.
- 629 Hernandez-Stefanoni, J.L., Gallardo-Cruz, J.A., Meave, J.A., Rocchini, D.,  
630 Bello-Pineda, J., López-Martínez, J.O., 2012. Modeling  $\alpha$ - and  $\beta$ -diversity  
631 in a tropical forest from remotely sensed and spatial data. *Int. J. Appl.*  
632 *Earth Observ. Geoinform.* 19, 359-368.
- 633 Hill, M.O., Gauch, H.G., 1980. Detrended correspondence analysis: an im-  
634 proved ordination technique. *Vegetatio* 42, 47–58.
- 635 Kohonen, T. (1982). Analysis of a simple self-organizing process. *Biological*  
636 *Cybernetics*, 44: 135-140.

- 637 Latombe, G., Hui, C., McGeoch, M.A. (2017) Multi-site generalised dissimi-  
638 larity modelling: using zeta diversity to differentiate drivers of turnover in  
639 rare and widespread species. *Methods in Ecology and Evolution*, 8, 431-  
640 442.
- 641 Lausch, A., Bannehr, L., Beckmann, M., Boehm, C., Feilhauer, H., Hacker,  
642 J.M., Heurich, M., Jung, A., Klenke, R., Neumann, C., Pause, M., Roc-  
643 chini, D., Schaepman, M.E., Schmidlein, S., Schulz, K., Selsam, P., Set-  
644 tele, J., Skidmore, A.K., Cord, A.F. (2016). Linking Earth Observation  
645 and taxonomic, structural and functional biodiversity: Local to ecosystem  
646 perspectives. *Ecological Indicators*, 70: 317-339.
- 647 Leathwick, J.R., Snelder, T., Chadderton, W.L., Elith, J., Julian, K., Ferrier,  
648 S. (2011). Use of generalised dissimilarity modelling to improve the biolog-  
649 ical discrimination of river and stream classifications. *Freshwater Biology*,  
650 56, 21-38.
- 651 Legendre, P., Borcard, D., Peres-Neto, P.R. (2005) Analyzing beta diver-  
652 sity: Partitioning the spatial variation of community composition data.  
653 *Ecological Monographs*, 75, 435-450.
- 654 Leitão, P.J., Schwieder, M., Suess, S., Catry, I., Milton, E.J., Moreira, F.,  
655 Osborne, P.E., Pinto, M.J., van der Linden, S., Hostert, P. (2015) Map-  
656 ping beta diversity from space: sparse generalised dissimilarity modelling  
657 (SGDM) for analysing high-dimensional data. *Methods in Ecology and*  
658 *Evolution*, 6, 764-771.
- 659 Leitão, P., Schwieder, M., Senf, C. (2017) *sgdm*: An R Package for Perform-  
660 ing Sparse Generalized Dissimilarity Modelling with Tools for *gdm*. *ISPRS*  
661 *International Journal of Geo-Information*, 6, 23.
- 662 Mantel, N., Valand, R.S. (1970) A technique of nonparametric multivariate  
663 analysis. *Biometrics*, 26, 547-558.
- 664 Mazor, T., Kark, S., Possingham, H.P., Rocchini, D., Levy, Y., Richardson,  
665 A.J., Levin, N. (2013). Can satellite-based night lights be used for conser-  
666 vation? The case of nesting sea turtles in the Mediterranean. *Biological*  
667 *Conservation*, 159: 63-72.
- 668 Meentemeyer, R.K., Anacker, B.L., Mark, W., Rizzo, D.M. (2008). Early  
669 detection of emerging forest disease using dispersal stimation and ecological  
670 niche modeling. *Ecological Applications*, 18: 377-390.

- 671 Metz, M., Rocchini, D., Neteler, M. (2014). Surface temperatures at the  
672 continental scale: tracking changes with remote sensing at unprecedented  
673 detail. *Remote Sensing*, 6: 3822-3840.
- 674 Moilanen, A., Franco, A.M.A., Early, R., Fox, R., Wintle, B., Thomas, C.D.  
675 (2005). Prioritizing multiple-use landscapes for conservation: methods for  
676 large multi-species planning problems. *Proceedings of the Royal Society B:  
677 Biological Sciences*, 272: 1885-1891.
- 678 Moilanen, A., Kujala, H., Leathwick, J.R. (2009). The zonation framework  
679 and software for conservation prioritization. in A. Moilanen, K. Wilson,  
680 H.P. Possingham (Eds.), *Spatial Conservation Prioritization: Quantitative  
681 Methods Computational Tools*, Oxford University Press (2009), pp. 196-  
682 210.
- 683 Neumann, C., Weiss, G., Schmidlein, S., Itzerott, S., Lausch, A., Doktor,  
684 D., Brell, M., 2015. Ecological gradient-based habitat quality assessment  
685 for spectralecosystem monitoring. *Remote Sens.* 7, 2871–2898.
- 686 Palmer, M.W., Earls, P.G., Hoagland, B.W., White, P.S., Wohlgemuth, T.,  
687 2002. Quantitative tools for perfecting species lists. *Environmetrics* 13,  
688 121–137. doi:10.1002/env.516
- 689 QGIS Development Team, 2016. QGIS Geographic Information System.  
690 Open Source Geospatial Foundation. <http://qgis.osgeo.org>
- 691 Randell, D., Turnbull, K., Ewans, K., Jonathan, P. (2016). Bayesian inference  
692 for nonstationary marginal extremes. *Environmetrics*, 27: 439-450.
- 693 Rocchini, D. (2007). Distance decay in spectral space in analysing ecosystem  
694  $\beta$ -diversity. *International Journal of Remote Sensing*, 28: 2635-2644.
- 695 Rocchini, D., Andreini Butini, S., Chiarucci, A. (2005). Maximizing plant  
696 species inventory efficiency by means of remotely sensed spectral distances.  
697 *Global Ecology and Biogeography*, 14: 431-437.
- 698 Rocchini, D., Balkenhol, N., Carter, G.A., Foody, G.M. Gillespie, T.W., He,  
699 K.S., Kark, S., Levin, N., Lucas, K., Luoto, M., Nagendra, H., Oldeland,  
700 J., Ricotta, C., Southworth, J., Neteler, M. (2010). Remotely sensed spec-  
701 tral heterogeneity as a proxy of species diversity: recent advances and open  
702 challenges. *Ecological Informatics*, 5: 318-329.
- 703 Rocchini, D., Boyd, D.S., Féret, J.B., Foody, G.M., He, K.S., Lausch, A.,  
704 Nagendra, H., Wegmann, M., Pettorelli, N. (2016). Satellite remote sensing

- 705 to monitor species diversity: potential and pitfalls. *Remote Sensing in*  
706 *Ecology and Conservation*, 2: 25-36.
- 707 Rocchini, D., Delucchi, L., Bacaro, G., Cavallini, P., Feilhauer, H., Foody,  
708 G.M., He, K.S., Nagendra, H., Porta, C., Ricotta, C., Schmidtlein, S.,  
709 Spano, L.D., Wegmann, M., Neteler, M. (2013). Calculating landscape  
710 diversity with information-theory based indices: A GRASS GIS solution.  
711 *Ecological Informatics*, 17: 82-93.
- 712 Rocchini, D., Garzon-Lopez, C.X., Marcantonio, M., Amici, V., Bacaro, G.,  
713 Bastin, L., Brummitt, N., Chiarucci, A., Foody, G.M., Hauffe, H.C., He,  
714 K.S., Ricotta, C., Rizzoli, A., Rosá, R. (2017). Anticipating species dis-  
715 tributions: handling sampling effort bias under a Bayesian framework.  
716 *Science of the Total Environment*, 584-585, 282-290.
- 717 Rocchini, D., Hernández Stefanoni, J.L., He, K.S: (2015). Advancing species  
718 diversity estimate by remotely sensed proxies: a conceptual review. *Eco-*  
719 *logical Informatics*, 25: 22-28.
- 720 Rocchini, D., Neteler, M. (2012). Let the four freedoms paradigm apply to  
721 ecology. *Trends in Ecology & Evolution*, 27: 310–311.
- 722 Rosauer, D.F., Ferrier, S., Williams, K.J., Manion, G., Keogh, J.S., Laffan,  
723 S.W. (2014) Phylogenetic generalised dissimilarity modelling: a new ap-  
724 proach to analysing and predicting spatial turnover in the phylogenetic  
725 composition of communities. *Ecography*, 37, 21-32.
- 726 Schmidtlein, S., Sassin, J., 2004. Mapping continuous floristic gradients  
727 in grasslands using hyperspectral imagery. *Remote Sens. Environ.* 92,  
728 126–138.
- 729 Schmidtlein, S., Zimmermann, P., Schüpferling, R., Weiss, C., 2007. Mapping  
730 the floristic continuum: ordination space position estimated from imaging  
731 spectroscopy. *Journal of Vegetation Science*, 18: 131–140.
- 732 Tuomisto, H., Poulsen, A., Ruokolainen, K., Moran, R., Quintana, C., Celi,  
733 J., Canas, G. (2003). Linking floristic patterns with soil heterogeneity and  
734 satellite imagery in Ecuadorian Amazonia. *Ecological Applications*, 13:  
735 352-371.
- 736 Tuomisto, H., Ruokolainen, K., 2006. Analyzing or explaining beta diversity?  
737 Understanding the targets of different methods of analysis. *Ecology* 87,  
738 2697–2708. doi:10.1890/0012-9658(2006)87[2697:AOEBDU]2.0.CO;2

- 739 Tyre, A.J., Possingham, H.P., Lindenmayer, D.B. (2001). Inferring process  
740 from pattern: can territory occupancy provide information about life his-  
741 tory parameters? *Ecological Applications*, 11: 1722-1737.
- 742 Tahvanainen, T. (2011). Abrupt ombrotrophication of a boreal aapa mire  
743 triggered by hydrological disturbance in the catchment. *Journal of Ecology*  
744 2011, 99: 404-415.
- 745 Ustin, S.L., Gamon, J.A., 2010. Remote sensing of plant functional types.  
746 *New Phytol.* 186, 795–816.
- 747 Vaglio Laurin, G., Chan, J.C.-W., Chen, Q., Lindsell, J.A., Coomes, D.A.,  
748 Guerriero, L., Frate, F.D., Miglietta, F., Valentini, R., 2014. Biodiversity  
749 Mapping in a Tropical West African Forest with Airborne Hyperspectral  
750 Data. *PLoS ONE* 9, e97910. doi:10.1371/journal.pone.0097910
- 751 Vernesi, C., Rocchini, D., Pecchioli, E., Neteler, M., Vendramin, G.G., Paf-  
752 fetti, D. (2012). A landscape genetics approach reveals ecological-based  
753 differentiation in populations of holm oak (*Quercus ilex*, L.) at their north-  
754 ernmost distribution edge. *Biological Journal of the Linnean Society*, 107:  
755 458-467.
- 756 Vihervaara, P., Auvinen, A.-P, Mononen, L., Törmä, M., Ahlroth, P.,  
757 Anttila, S., Böttcher, K., Forsius, M., Heino, J., Heliölä, J., Koskelainen,  
758 M., Kuussaari, M., Meissner, K., Ojala, O., Tuominen, S., Viitasalo, M.,  
759 Virkkala, R. 2017: How Essential Biodiversity Variables and remote sens-  
760 ing can help national biodiversity monitoring. *Global Ecology and Conser-  
761 vation* 10: 43-59.
- 762 Wegmann, M. Leutner, B.F., Metz, M., Neteler, M., Dech, S., Rocchini,  
763 D. (2017). r.pi: a GRASS GIS package for semi-automatic spatial pat-  
764 tern analysis of remotely sensed land cover data. *Methods in Ecology and  
765 Evolution*.
- 766 Whittaker, R.H. (1960) Vegetation of the Siskiyou Mountains, Oregon and  
767 California. *Ecological Monographs*, 30, 280-338.
- 768 Witten, D., Tibshirani, R., Gross, S., Narasimhan, B. (2013) PMA: Penalized  
769 Multivariate Analysis.
- 770 Woolley, S.N.C., Foster, S.D., O'Hara, T.D., Wintle, B.A., Dunstan, P.K.  
771 (2017) Characterising uncertainty in generalised dissimilarity models.  
772 *Methods in Ecology and Evolution*, 8, 985-995.
- 773 Figures



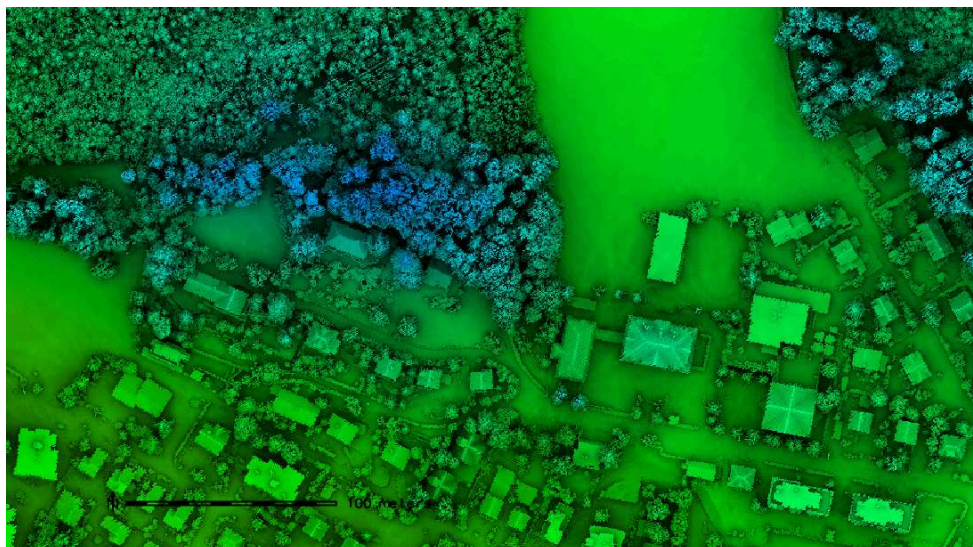


Figure 1: An example of how to couple information on compositional properties of the landscape by optical data together with structural (3D) properties by laser scanning LiDAR data.

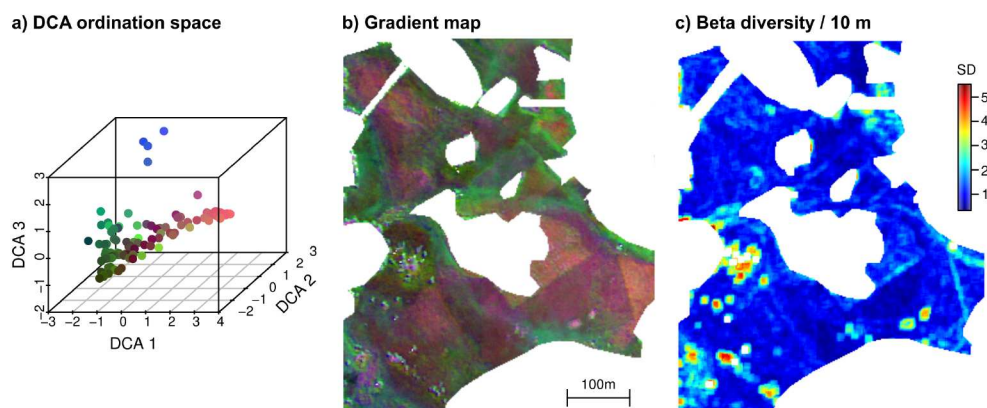


Figure 2:  $\beta$ -diversity assessment with a combination of ordination techniques and remote sensing. a) Three dimensional DCA ordination space of  $n=100$  vegetation plots sampled in raised bogs, fens, transition mires and *Molinia* meadows in the alpine foothills of Southern Germany. An inter-plot distance of 4 SD corresponds to a full species turnover. b) Maps of the ordination axes resulting from a spatial prediction based on canopy reflectance. Each pixel has a predicted position in the ordination space that is indicated by its color. The color scheme corresponds to a). The map has a spatial resolution of 2 m x 2 m, which is in line with the sampled plot size. c) Cumulative change rates along the three DCA axes in a 5 x 5 pixel neighborhood. A high change rate indicates a high beta diversity.

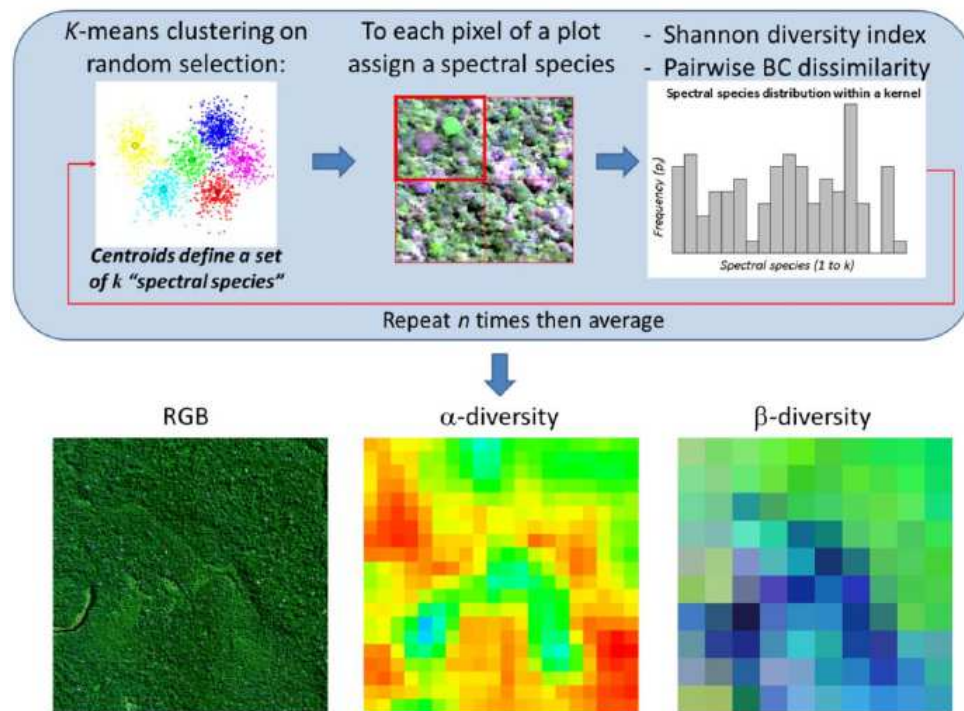


Figure 3: Spectral species can be identified in a hyper- or multi-spectral image by spatial clustering method and their distribution can be mapped. Such maps can further be used to apply local-based heterogeneity measurements ( $\alpha$ -diversity) as well as iterative distance based methods to build  $\beta$ -diversity maps. Reproduced from Féret and Asner (2014a).

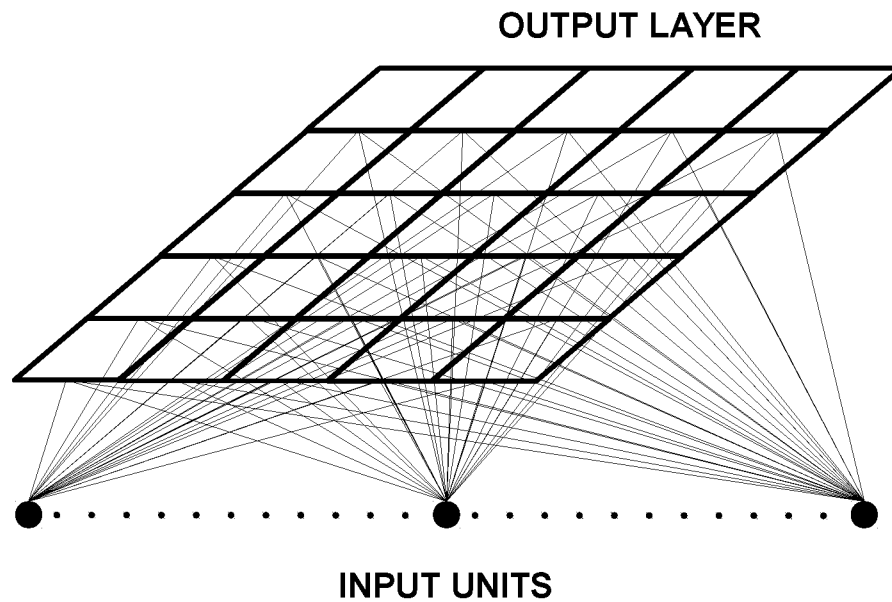


Figure 4: A self-organising feature map can be built starting from an input layer, e.g. the presence absence of a tree species or of a peculiar spectral value) which is connected to every unit in the output layer by a weighted connection. The self organising feature map uses unsupervised learning to map the location of field sites within the output space on the basis of their relative similarity in species or spectral composition. [Redrawn](#) from Foody and Cutler (2003).

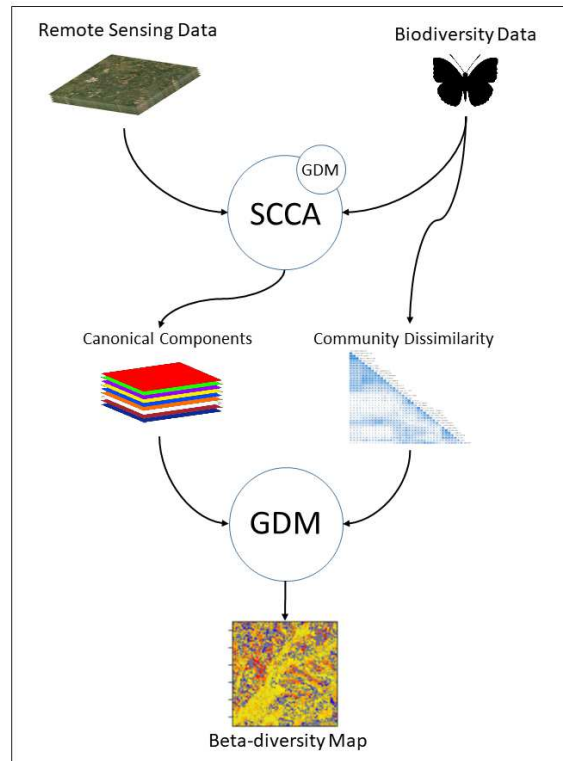


Figure 5: An example of the Sparse Generalized Dissimilarity Model (SGDM) approach. Remote sensing data and biodiversity data in the field can be coupled by Sparse Canonical Correlation Analysis to produce canonical components and a community dissimilarity matrix, which are then used to build a Generalized Dissimilarity Model to finally derived a  $\beta$ -diversity map.

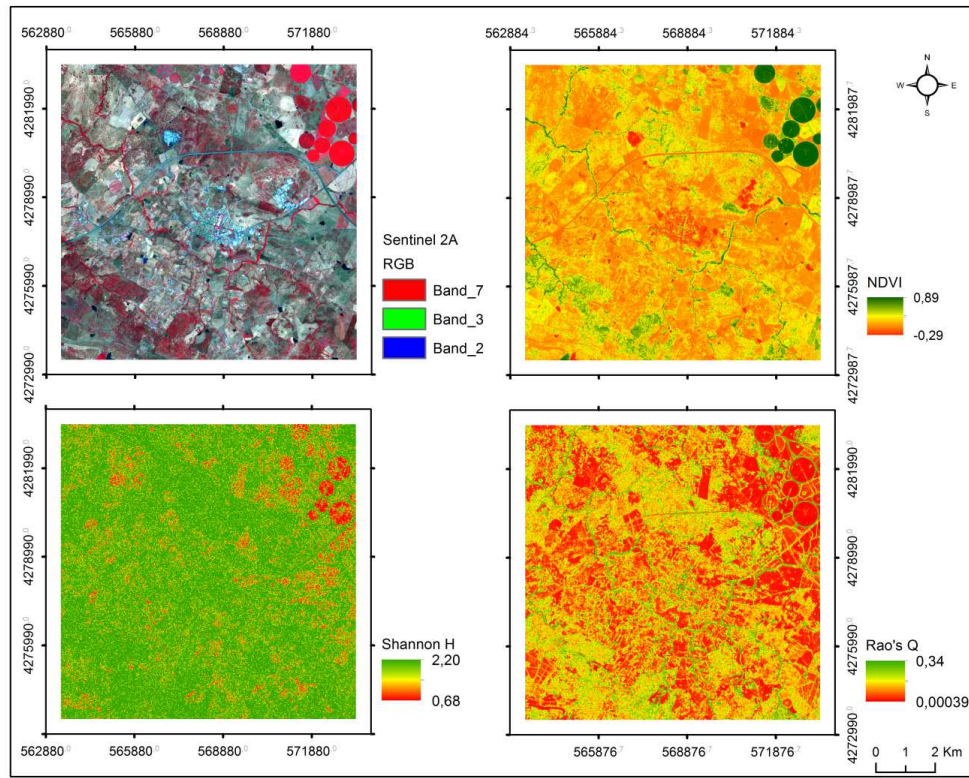


Figure 6: Upper panels: Sentinel-2A scene (8 August 2016) and derived NDVI for the agro-forestry systems test site located in southern Portugal. Lower panels: results from Shannon's H and Rao's Q indices computation. Shannon index tends to overestimate the landscape diversity when compared to the Rao's Q index.



1 Measuring  $\beta$ -diversity by remote sensing: a  
2 challenge for biodiversity monitoring

3 Duccio Rocchini <sup>1,2,3,\*</sup>, Sandra Luque <sup>4</sup>, Nathalie Pettorelli <sup>5</sup>,  
Lucy Bastin <sup>6,7</sup>, Daniel Doktor <sup>8</sup>, Nicolás Faedi <sup>3,9</sup>,  
Hannes Feilhauer <sup>10</sup>, Jean-Baptiste Féret <sup>4</sup>, Giles M. Foody <sup>11</sup>,  
Yoni Gavish <sup>12</sup>, Sergio Godinho <sup>13</sup>, William E. Kunin <sup>14</sup>,  
Angela Lausch <sup>8</sup>, Pedro J. Leitão <sup>15,16</sup>, Matteo Marcantonio <sup>17</sup>,  
Markus Neteler <sup>18</sup>, Carlo Ricotta <sup>19</sup>, Sebastian Schmidlein <sup>20</sup>,  
Petteri Vihervaara<sup>21</sup>, Martin Wegmann <sup>22</sup>,  
Harini Nagendra <sup>23</sup>

4 November 1, 2017

5 <sup>1</sup> Center Agriculture Food Environment, University of Trento, Via E.  
6 Mach 1, 38010 S. Michele all'Adige (TN), Italy

7 <sup>2</sup> Centre for Integrative Biology, University of Trento, Via Sommarive,  
8 14, 38123 Povo (TN), Italy

9 <sup>3</sup> Fondazione Edmund Mach, Research and Innovation Centre, Depart-  
10 ment of Biodiversity and Molecular Ecology, Via E. Mach 1, 38010 S. Michele  
11 all'Adige (TN), Italy, corresponding author: ducciorocchini@gmail.com, duc-  
12 cio.rocchini@fmach.it

13 <sup>4</sup> UMR-TETIS, IRSTEA Montpellier, Maison de la Télédétection, 500  
14 rue JF Breton, 34093, Montpellier Cedex 5, France

15 <sup>5</sup> Institute of Zoology, The Zoological Society of London, Regent's Park,  
16 London, United Kingdom

17 <sup>6</sup> School of Computer Science, Aston University, United Kingdom

18 <sup>7</sup> Currently on secondment to Knowledge Management Unit, Joint Re-  
19 search Centre of the European Commission, Italy

20 <sup>8</sup> Helmholtz Centre for Environmental Research - UFZ, Department Com-  
21 putational Landscape Ecology Permoserstrasse 15, 04318 Leipzig, Germany

22 <sup>9</sup> Department of Computer Science and Engineering, University of Bologna,  
23 Mura Anteo Zamboni, 7, 40126 Bologna, Italy



24 <sup>10</sup> Institut für Geographie Friedrich-Alexander Universität Erlangen-Nürnberg  
25 Wetterkreuz 15, 91058 Erlangen, Germany

26 <sup>11</sup> School of Geography, University of Nottingham, Nottingham, NG7  
27 2RD, United Kingdom

28 <sup>12</sup> School of Biology, Faculty of biological Science, University of Leeds,  
29 Leeds LS2 9JT, United Kingdom

30 <sup>13</sup> Universidade de Evora , Evora · Institute of Mediterranean Agricultural  
31 and Environmental Sciences (ICAAM)

32 <sup>14</sup> School of Biology, University of Leeds, Leeds, UK

33 <sup>15</sup> Department Landscape Ecology and Environmental System Analy-  
34 sis, Technische Universität Braunschweig, Langer Kamp 19c, 38106 Braun-  
35 schweig, Germany

36 <sup>16</sup> Geography Department, Humboldt-Universität zu Berlin, Unter den  
37 Linden 6, 10099 Berlin, Germany

38 <sup>17</sup> Department of Pathology, Microbiology, and Immunology, School of  
39 Veterinary Medicine, University of California, Davis, USA

40 <sup>18</sup> Mundialis GmbH & Co. KG, Kölnstraße 99, 53111 Bonn, Germany

41 <sup>19</sup> Department of Environmental Biology, University of Rome “La Sapienza”,  
42 00185 Rome, Italy

43 <sup>20</sup> Karlsruher Institut für Technologie (KIT), Institut für Geographie und  
44 Geoökologie, Kaiserstr. 12, 76131 Karlsruhe, Germany

45 <sup>21</sup> Finnish Environment Institute (SYKE), Natural Environment Centre  
46 Mechelininkatu 34a,P.O.Box 140 FI-00251 Helsinki, Finland

47 <sup>22</sup> Department of Remote Sensing, Remote Sensing and Biodiversity Re-  
48 search Group, University of Wuerzburg, Wuerzburg, Germany

49 <sup>23</sup> Azim Premji University, PES Institute of Technology Campus, Pixel  
50 Park, B Block, Electronics City, Hosur Road, Bangalore, 560100, India

## 51 **Abstract**

52 Biodiversity includes multiscalar and multitemporal structures and  
53 processes, with different levels of functional organization, from genetic  
54 to ecosystemic levels. One of the mostly used methods to infer bio-  
55 diversity is based on taxonomic approaches and community ecology  
56 theories. However, gathering extensive data in the field is difficult due  
57 to logistic problems, [especially](#) when aiming at modelling biodiversity  
58 changes in space and time, which assumes statistically sound sampling  
59 schemes. In this [context](#), [airborne](#) or satellite remote sensing allow [in-](#)  
60 [formation to be gathered](#) over wide areas in a reasonable time.

61 Most of the biodiversity maps obtained from remote sensing have  
62 been based on the inference of species richness by regression analy-  
63 sis. On the contrary, estimating compositional turnover ( $\beta$ -diversity)

64 might add crucial information related to relative abundance of dif-  
65 ferent species instead of just richness. Presently, few studies have  
66 addressed the measurement of species compositional turnover from  
67 space.

68 Extending on previous work, in this manuscript we propose novel  
69 techniques to measure  $\beta$ -diversity from airborne or satellite remote  
70 sensing, mainly based on: i) multivariate statistical analysis, ii) the  
71 spectral species concept, iii) self-organizing feature maps, iv) multi-  
72 dimensional distance matrices, and the v) Rao's Q diversity. Each  
73 of these measures addresses one or several issues related to turnover  
74 measurement. This manuscript is the first methodological example  
75 encompassing (and enhancing) most of the available methods for es-  
76 timating  $\beta$ -diversity from remotely sensed imagery and potentially  
77 relating them to species diversity in the field.

78 *Keywords:*  $\beta$ -diversity, Kohonen self-organising feature maps, Rao's Q  
79 diversity index, remote sensing, satellite imagery, Sparse Generalized Dis-  
80 similarity Model, spectral species concept.

## 81 1 Introduction

82 Biodiversity cannot be fully investigated without considering the spatial com-  
83 ponent of its variation. In fact, it is known that the dispersal of species over  
84 wide areas is driven by spatial constraints directly related to the distance  
85 among sites. A negative exponential dispersal kernel is usually adopted to  
86 mathematically describe the occupancy of new sites by species, as:

$$F = \sum_{K=1}^N e^{\frac{-d_{ik}}{a}} \quad (1)$$

87 where  $d_{ik}$  = distance between two locations  $i$  and  $k$  and  $a$  is a parameter  
88 regulating the dispersal from localized areas (low values of  $a$ ) to widespread  
89 ones (high values of  $a$ , Meentemeyer et al. (2008)).

90 In this sense, distance acquires a significant role in ecology to estimate bio-  
91 diversity change. Hence, spatially explicit methods have been acknowledged  
92 in ecology for providing robust estimates of diversity at different hierarchical  
93 levels: from individuals (Tyre et al., 2001), to populations (Vernesi et al.,  
94 2012), to communities (Rocchini et al., 2005).

95 When dealing with spatial explicit methods, remote sensing images repre-  
96 sent a powerful tool, particularly when coupling information on compositional  
97 properties of the landscape with its structure (Figure 1). Remote sensing has

98 widely been used for conservation practices including very different types of  
99 data such as nightlights data (Mazor et al., 2013), Land Surface Temperature  
100 estimated from MODIS data (Metz et al., 2014), spectral indices (Gillespie,  
101 2005).

102 Most of the remote sensing applications for biodiversity estimation have  
103 relied on the estimate of local diversity hotspots, considering land use diver-  
104 sity (Wegmann et al., 2017) or continuous spatial variability of the spectral  
105 signal (Rocchini et al., 2010). This is mainly grounded in the assumption  
106 that a higher landscape heterogeneity is strictly related to a higher amount  
107 of species occupying different niches. However, given two sites  $s_1$  and  $s_2$ , the  
108 final diversity is not only related to the species / spectral richness of  $s_1$  and  
109  $s_2$ , but overall to the amount of shared species / spectral values. In other  
110 words, the lower the their intersection  $s_1 \cap s_2$ , the higher will be the total  
111 diversity, while a low total diversity will be reached when  $s_1 \cap s_2 = s_1 \cup s_2$ .  
112 Such intersection has been widely studied in ecology, after the development  
113 of  $\beta$ -diversity theory (Whittaker, 1960).

114 Tuomisto et al. (2003) demonstrated the power of substituting distance in  
115 Eq. 1 by spectral distance to directly account for the distance between sites  
116 in an environmental space, instead of a merely spatial one. However, while  
117 spectral distance examples exist when measuring the  $\beta$ -diversity among pairs  
118 of sites (e.g. Rocchini et al. (2015)), few studies have tested the possibility of  
119 measuring  $\beta$ -diversity over wide areas considering several sites at the same  
120 time (however see Alahuhta et al. (2017); Harris et al. (2015)). This is  
121 especially true when considering the development of remote sensing tools  
122 for diversity estimate in which the concept of  $\beta$ -diversity is still pioneering.

123 The aim of this paper is to present the most novel methods to measure  
124  $\beta$ -diversity from remotely sensed imagery based on the the most recently  
125 published ecological models. In particular we will deal with: i) multivariate  
126 statistical techniques, ii) the applicability of the spectral species concept,  
127 iii) multidimensional distance matrices, iv) metrics coupling abundance and  
128 distance-based measures.

129 This manuscript is the first methodological example encompassing (and  
130 enhancing) most of the available methods for estimating  $\beta$ -diversity from  
131 remotely sensed imagery and potentially relate them to species diversity in  
132 the field.

## 133 2 Multivariate statistical analysis for species 134 diversity estimate from remote sensing

135 Univariate statistics have been used to directly find relations between spectral  
136 and species diversity. However, the amount of variability explained by single  
137 bands / vegetation indices versus species diversity is generally relatively low,  
138 due to the fact that different aspects related to the complexity of habitats  
139 might act in shaping diversity, from disturbance and land use at local scales  
140 to climate and element fluxes at global scales.

141 Ordination techniques are designed to quantitatively describe multivari-  
142 ate gradual transitions in the species composition of sampled sites. Measuring  
143 the distance between two sampling sites in the multi-dimensional ordination  
144 space is a good proxy of the change in species composition. When this mea-  
145 sure is related to the geographical distance between the considered sites, the  
146 beta diversity at this particular scale can be assessed.

147 Of the various available ordination techniques, Detrended Correspon-  
148 dence Analysis (DCA, Hill and Gauch (1980)) is particularly suitable for  
149 such analyses. The axes (i.e. gradients) of the DCA ordination space are  
150 scaled in standard deviation (SD) units, where a distance of 4 SD is related  
151 to a full species turnover. This enables a versatile analysis that easily reveals  
152 whether two sampled sites still have species in common.

153 Several studies have mapped the ordination space using remote sensing  
154 data (e.g., Schmidtlein and Sassini (2004); Schmidtlein et al. (2007); Feil-  
155 hauer et al. (2009, 2011, 2014); Gu et al. (2015); Harris et al. (2015); Leitao  
156 et al. (2015); Neumann et al. (2015)). For this purpose, the axes scores of  
157 the sampled sites are regressed against the corresponding canopy reflectance  
158 values extracted from air- or spaceborne image data. The resulting multi-  
159 variate regression models, one per ordination axis and most often generated  
160 with machine learning regression techniques, are subsequently applied on the  
161 image data for a spatial prediction of ordination scores. Each pixel of the  
162 image data is assigned to a specific position in the ordination space that in-  
163 dicates its species composition. The resulting gradient maps are a powerful  
164 tool for analyses of beta diversity across different spatial scales (Feilhauer et  
165 al., 2009; Hernandez-Stefanoni et al., 2012).

166 A simple analysis of the variability of the DCA scores in a defined pixel  
167 neighborhood (i.e. a moving window) results in a efficient beta diversity  
168 assessment. The spatial scale of this assessment can be varied either by  
169 re-sampling the gradient map to a coarser spatial resolution (i.e. pixel size) or  
170 by changing the kernel size of the considered pixel neighborhood. Such tech-  
171 niques have been further developed e.g. for spatial conservation prioritization

172 programmes such as [Zonation](#) (Moilanen et al., 2005, 2009).

173 Figure 2 shows an example of a DCA-based assessment of beta diversity  
174 on a very local scale (10 m) following the approach described in Feilhauer et  
175 al. (2009). The analyzed landscape is a mosaic of raised bogs, fens, transition  
176 mires and *Molinia* meadows. For a detailed description of the data and site  
177 please refer to Feilhauer et al. (2014, 2016).

178 Analyses like this require two different data sets: (1) a sample of field  
179 data that is representative for the vegetation in the studied area and is used  
180 to generate the ordination space; (2) image data with a sufficient spectral  
181 resolution to discriminate the vegetation types within the ordination space  
182 and with a spatial resolution that is in line with the sampling design of the  
183 field data (Feilhauer et al., 2013).

184 Using these data, the continuous spatial variability of the spectral signal  
185 in the image pixels is translated into a spatially continuous measure of species  
186 composition. The advantages of this approach are obvious: since the diversity  
187 analyses are conducted in the floristic gradient space, the resulting measures  
188 resemble field studies and are thus easier to interpret than spectral proxies  
189 and closer to the point of view of many end-users. [Furthermore](#), the analysis  
190 of ordination scores in defined pixel neighborhoods is not restricted to a  
191 single spatial scale but offers the opportunity to implement assessments of  
192 beta diversity on multiple scales.

### 193 **3 The spectral species concept**

194 The spectral species concept has been proposed by Féret and Asner (2014a)  
195 to map both  $\alpha$  and  $\beta$  component of the biodiversity using a unique frame-  
196 work. It is rooted in the convergence between two other concepts, the spec-  
197 tral variation hypothesis (SVH) proposed by Palmer et al. (2002), and the  
198 plant optical types proposed by Ustin and Gamon (2010), sustained by the  
199 technological advances in the domain of high spatial resolution imaging spec-  
200 troscopy. The SVH states that the spatial variability in the remotely sensed  
201 signal, that is the spectral heterogeneity, is related to environmental hetero-  
202 geneity and could therefore be used as a powerful proxy of species diversity.  
203 SVH has been tested in different situations (Rocchini et al., 2010) and con-  
204 clusions show that the [performance](#) of this approach is very dependent on  
205 several factors, including the [instrument](#) characteristics (spectral, spatial and  
206 temporal resolution), the type of vegetation investigated, and the metrics de-  
207 rived from remotely sensed information to estimate spectral heterogeneity.  
208 Plant optical types refer to the capacity of sensors to measure [signals that](#)  
209 [aggregate](#) information about vegetation structure, phenology, biochemistry

210 and physiology. Therefore, this concept is also tightly linked to the perfor-  
211 mances of the sensor and finds particular echo with the increasing use of high  
212 spatial resolution imaging spectroscopy for the estimation and identification  
213 of multiple vegetations properties.

214 The details provided by high spatial resolution imaging spectroscopy are  
215 sufficient to perform analyses of plant optical traits at the individual tree scale  
216 in order to differentiate tree species, obtain information about leaf chemical  
217 traits and estimate the  $\alpha$  component of biodiversity (Asner et al., 2008, 2015;  
218 Chadwick and Asner, 2016; Clark et al., 2005; Clark and Roberts, 2012;  
219 Féret and Asner, 2013; Vaglio Laurin et al., 2014). These results illustrate  
220 that spectral information can be related to taxonomic or functional informa-  
221 tion of the vegetation, which supports the SVH under the hypothesis that  
222 the metrics used to compute spectral heterogeneity and a given component  
223 of vegetation diversity are properly defined. However these applications are  
224 currently limited by the important amount of field data required to train re-  
225 gression or classification models, which is also directly linked to their low ge-  
226 neralization ability in time and space. Unsupervised approaches then appear  
227 as valuable alternatives for the analysis of ecosystem heterogeneity (Baldeck  
228 and Asner, 2013; Baldeck et al., 2014; Feilhauer et al., 2011; Baldeck and  
229 Asner, 2013; Féret and Asner, 2014b), as ecological indicators of  $\alpha$  and  $\beta$   
230 diversity at landscape scale usually require one or several levels of abstraction  
231 beyond the correct taxonomic identification (Tuomisto et al., 2006).

232 Clustering (properly pre-processed) spectral information should result in  
233 pixels from the same species naturally grouping together rather than dis-  
234 tributing randomly among clusters, Féret and Asner (2014a) proposed a  
235 grouping method aiming at assigning labels to pixels based on multiple clus-  
236 tering of spectroscopic data acquired at landscape scale. These pixels, labeled  
237 with a set of so-called spectral species, can then be used straightforwardly  
238 in order to compute various diversity metrics such as Shannon index for  $\alpha$   
239 diversity, and Bray-Curtis dissimilarity for  $\beta$  diversity. The pre-processing  
240 stage is divided into several stages. After masking all non-vegetated pixels, a  
241 normalization based on **continuous** removal is applied to each pixel and over  
242 the full spectral domain, then a principal component analysis is performed on  
243 the **continuously** removed spectral data. The normalization **reduces** effects  
244 due to changes in illumination, canopy geometry and other factors unrelated  
245 to vegetation, while enhancing the signal corresponding to vegetation. The  
246 components including individual-specific information are the components of  
247 interest. They can be identified after visual inspection or automated routines,  
248 if initial data show sufficient signal to noise ratio. Once a limited number  
249 of components have been selected, k-means clustering is then applied to a  
250 certain number of subsets, and for each of these subsets, centroids are com-

251 puted and each pixel in the image is labeled based on the closest centroid.  
252 The repetition of clustering based on various subsets of the image tends to  
253 minimize the risk of assigning centroids to irrelevant groups of pixels. Ex-  
254 perimental results showed that the averaging of diversity indices computed  
255 from multiple centroid maps can be seen as an analogous to signal averaging,  
256 which consists in increasing signal to noise ratio by replicating measurements.  
257 For each repetition, the closest centroid corresponds to the spectral species,  
258 and for each spatial unit of a given size, the spectral species distribution is  
259 derived in order to compute any diversity metric requiring either information  
260 at the local scale, or comparison of information across spatially distant plots.

261 The concepts of spectral species and spectral species distribution have  
262 been tested successfully on a limited number of situations and types of  
263 ecosystems (see (Rocchini et al., 2016) for a review, and (Lausch et al.,  
264 2016) for an application to similar concepts). As an example, F eret and  
265 Asner (2014a) showed ability to properly estimate landscape heterogeneity  
266 at moderate spatial scale, up to few dozen square kilometers over tropical  
267 forests, based on high spatial resolution imaging spectroscopy (Figure 3).  
268 A generic parameterization of the method showed robust performances for  
269  $\alpha$  diversity mapping across space and time, but mapping  $\beta$  diversity across  
270 large spatial scales using images acquired during different airborne campaign  
271 remains challenging, which leads to an unsolved problem when considering  
272 operational regional mapping. In the perspective of global monitoring of  
273 biodiversity, and given the unprecedented remote sensing capacity allowed  
274 by the Copernicus program, including the Sentinel-2 multispectral satellites,  
275 several other challenges are foreseen and currently investigated. The influ-  
276 ence of decreased spatial and spectral resolution on the ability to properly  
277 differentiate ecologically meaningful spectral species across landscapes and  
278 over regions will need to be investigated. The application of this concept be-  
279 yond tropical forests and savanna ecosystems should also be investigated, as  
280 it may not hold when applied on moderately diverse ecosystems or systems  
281 with individuals whose individuals have dimensions well below the resolving  
282 power of the instrument.

## 283 4 Self organizing feature maps

284 The Kohonen self-organising feature map (SOFM, Kohonen (1982)) is a neu-  
285 ral network that may be used to undertake unsupervised clustering of data.  
286 Critically, the input to a SOFM can be a large multi-variate data set such  
287 as may be acquired on species from quadrat based field surveys. The SOFM  
288 summarises the data in a low, typically two, dimensional output (Figure



289 4). In this output space the data for individual quadrats are topologically  
290 ordered – with sites that are similar close together while those of highly dif-  
291 ferent species composition are more distant. Because the data sites in the  
292 output space are arranged by relative similarity the output space may also  
293 be used to aggregate or classify a data set. As such the SOFM is attrac-  
294 tive as a non-parametric clustering analysis and as a means to undertake an  
295 ordination (Chon et al., 1996).

296 A SOFM is, unlike some of the approaches used commonly in community  
297 ecology, not constrained by assumptions relating the statistical distribution  
298 of the data used. The SOFM uses unsupervised learning to produce a topo-  
299 logically ordered output space in which the samples are arranged spatially  
300 in relation to their relative similarity in species composition. The SOFM  
301 thus performs a non-parametric ordination analysis (Foody, 1999). The pro-  
302 duction of a classification by a SOFM comprises two main stages (Giraudel  
303 and Lek, 2001). An iterative analysis, in which time-decaying parameters  
304 that control network learning and the size of local neighbourhoods located  
305 around output units, is used. For this, the user must specify a number of key  
306 parameters such as the size and shape of the network, number of iterations of  
307 the algorithm, the learning rate and its rate of decline and a neighbourhood  
308 parameter. The need for such parameters can add some uncertainty to the  
309 analysis. While there are no formal rules to follow in the design of a SOFM  
310 there are recommendations for the determination of SOFM parameter set-  
311 tings (Giraudel and Lek, 2001). A further concern is that as an unsupervised  
312 classifier the classes defined may not always be the most useful for an in-  
313 vestigation. In addition, the nature of the analysis means the direction of  
314 the gradients cannot be controlled (Fritzke, 1995) but the analysis performs  
315 well in comparison to popular ordination techniques such as PCA and DCA  
316 (Foody and Cutler, 2003). The SOFM may also use a variety of different  
317 data types such as presence/absence, abundance or importance values and  
318 can solve complex non-linear problems (Giraudel and Lek, 2001).

## 319 5 Multidimensional distance matrices: GDMs 320 and SGDMs

321 One of the most widespread methods for assessing  $\alpha$ -diversity is using distance  
322 matrices (Legendre et al., 2005). Indeed, early work by Whittaker (1960) sug-  
323 gested that  $\beta$ -diversity could be quantified by dissimilarity matrices among  
324 (pairs of) sites. Furthermore, the Mantel test (Mantel and Valand, 2017),  
325 designed to estimate the association between two independent dissimilarity

326 matrices, has been widely used to correlate a community composition dissim-  
327 ilarity matrix with an environment dissimilarity one, thus providing useful  
328 insights into community composition and turnover (Legendre et al., 2005;  
329 Tahvanainen et al., 2011).

330 Generalized Dissimilarity Modelling (GDM; Ferrier (2007) can be con-  
331 sidered as an extension of the Mantel test, which is able to accommodate  
332 multidimensional environmental data, to be compared with the composi-  
333 tional data. GDMs also allow for the prediction of compositional turnover  
334 as well as for, e.g. environmental classification constrained to the compo-  
335 sitional dissimilarity (Ferrier, 2007; Leathwick et al., 2011). In GDM, the  
336 compositional dissimilarities between all pairs of samples are modelled as a  
337 function of their respective environmental distances. This is done through a  
338 linear combination of monotonic I-spline basis functions, under the assump-  
339 tion that increasing environmental dissimilarity (e.g. along a gradient) can  
340 only result in increasing compositional dissimilarity. This method is thus well  
341 suited for measuring and mapping  $\beta$ -diversity, and is thus becoming widely  
342 used in conservation science and macroecology, and recently been subject to  
343 several developments as we describe below.

344 One such development is the phylogenetic GDM (phylo-GDM; Rosauer  
345 et al. (2014)), which incorporates phylogenetic dissimilarities into GDM and  
346 allows for analysing and predicting phylogenetic  $\beta$ -diversity, thus linking  
347 ecological and evolutionary processes. This method can provide novel in-  
348 sights into the mechanisms underlying current patterns of biological diversity  
349 (Graham et al., 2008). Another recent development of GDM is the multi-  
350 site GDM (MS-GDM; Latombe et al. (2017)), which extends GDMs from  
351 pairwise to multi-site dissimilarity modelling. In such paper, the authors  
352 tested MS-GDM by means of both constrained (monotonical) additive mod-  
353 els and I-splines, although with no conclusive results relating to the best  
354 method overall. They concluded, however, that when applying MS-GDM to  
355 a high number of samples, they could better explain the drivers of species  
356 turnover. Also, an important development of GDM is the Bayesian bootstrap  
357 GDM (BBGDM; Woolley et al. (2017)) designed to characterize uncertainty  
358 in generalized dissimilarity models. This approach allows better represent-  
359 ing the underlying uncertainty in the data, by estimating the variance in  
360 parameters based on the available data.

361 Finally, an implementation of GDM, which was created particularly for  
362 dealing with high-dimensional (and potentially high-collinear) remote sensing  
363 data as input in GDM is the Sparse Generalized Dissimilarity Model (SGDM,  
364 Figure 5, Leitao et al. (2015)). This method is a two-stage approach that  
365 consists of initially reducing the environmental space (e.g. reflectance data)  
366 by means of a Sparse Canonical Correlation Analysis (SCCA, Figure 5; Wit-

ten et al. (2013)), and then fitting the resulting components with a GDM model. The SCCA is a form of penalized canonical correlation analysis based on the L1 (lasso) penalty function, and is thus designed to deal with high-dimensional data. The two algorithms are coupled in a way that the SCCA penalization is selected through a heuristic grid search manner, in order to minimize the cross-validate root mean square error in the dissimilarities predicted by the GDM. In this procedure, the high-dimensional environmental data (such as coming from time series of multispectral or hyperspectral data) are subject to a supervised ordination approach that reduces their dimension while capturing the axes of variation that most correlate to those of the community compositional matrix. SGDM has been successfully used for modelling and mapping the compositional turnover of both animal and plant species, using several different sources of remote sensing (and auxiliary) data (Leitao et al., 2015; Leitão et al., 2017).

## 6 Rao's Q diversity

Most of the previously shown metrics are based on the distance among pixel values in a multidimensional spectral space. None of them considers the relative abundance of such pixel values in a neighbourhood.

By contrast, abundance-based metrics such as the Shannon entropy could output similar results despite a variable distance among pixel values. As an example, consider a 3x3 matrix of remotely sensed data:

$$\begin{pmatrix} x_{11} & x_{12} & x_{13} \\ x_{21} & x_{22} & x_{23} \\ x_{d1} & x_{d2} & x_{d3} \end{pmatrix} \quad (2)$$

composed by the following values:

$$\begin{pmatrix} 10 & 13 & 15 \\ 18 & 20 & 23 \\ 19 & 21 & 22 \end{pmatrix} \quad (3)$$

then consider a different matrix:

$$\begin{pmatrix} 10 & 121 & 227 \\ 1 & 40 & 251 \\ 7 & 100 & 149 \end{pmatrix} \quad (4)$$

From a Shannon's entropy perspective, such matrices are equal in terms of heterogeneity. The Shannon's entropy is indeed based on the relative abundance (and richness) of a sample, and its value is 2.197 for both the matrices.

393 This value, equalling the natural logarithm of the number of classes (pixel  
394 values), is also Shannon's maximum theoretical value given a 3x3 matrix,  
395 due to the lack of identical numbers in the matrices. This example explicitly  
396 shows that accounting for the distance among values and their relative abun-  
397 dance is crucial to discriminate among areas in terms of measured (modeled)  
398 heterogeneity.

399 One of the metrics accounting for both the abundance and the pairwise  
400 spectral distance among pixels is the Rao's Q diversity index, as:

$$Q = \sum \sum d_{ij} \times p_i \times p_j \quad (5)$$

401 where  $d_{ij}$  = spectral distance among pixels  $i$  and  $j$  and  $p$  = proportion of  
402 occupied area.

403 Hence, Rao's Q is capable of discriminating among the ecological diversity  
404 of matrices 3 and 4, turning out to be 4.59 and 90.70, respectively. Appendix  
405 1 provide an example spreadsheet to perform the calculation while the com-  
406 plete R code is stored in the GitHub repository  
407 <https://github.com/mattmar/spectralrao>.

408 We decided to make use of a case study to highlight the importance of  
409 considering the distance among pixel values in remote sense ecological appli-  
410 cation. The performance of Rao's Q index in describing landscape diversity  
411 was tested in a complex agro-forestry landscape located in southern Portu-  
412 gal. A test site with an area of about  $10 \times 10 \text{ km}^2$  (centroid located at  $38^\circ$   
413  $39' 10.74''$  N;  $8^\circ 12' 52.30''$  W) was selected to conduct the analysis. In this  
414 area, a savanna-like ecosystem called montado occupies about 40% of the test  
415 site, followed by traditional olive groves, pastures, vineyards, and irrigated  
416 monocultures (e.g. corn fields). Montado is spatially characterized by the  
417 variability of its tree density (e.g. Godinho et al. (2016)), and the gradient  
418 between low and high tree density over space can lead to different structural  
419 heterogeneity and habitat diversity.

420 Within the test site, polyculture under small farming context (e.g. veg-  
421 etable gardens, orchards, and cereal crops) is an important feature of this  
422 landscape by generating a high compositional and configurational spatial  
423 heterogeneity (Figure 6). The main goal in using this case study is to demon-  
424 strate the potential and effectiveness of the Rao's Q index in producing ac-  
425 curately remote-sensing based maps of spatial diversity over such complex  
426 landscape. For this study, a cloud-free Sentinel-2A (S2A) image acquired  
427 on 8 of August 2016 was used to compute the NDVI at a 10 meters spatial  
428 resolution. The S2A image download, as well as the atmospheric correction  
429 (DOS method) were performed using the Semi-Automatic Classification plu-  
430 gin (SCP) implemented in the QGIS software (QGIS Development Team ,  
431 2016(@)).

432 The NDVI was used as input data for Rao's Q index computation using  
433 a window size of  $3 \times 3$  pixels. The performance of the Rao's Q was compared  
434 to the Shannon Entropy index (Shannon's H), which is one of the simplest,  
435 and widely used, remote sensing-based diversity measures for landscape het-  
436 erogeneity assessment (Rocchini et al., 2016). To investigate whether both  
437 diversity indices differ between land cover types, one-way ANOVA tests were  
438 performed. This approach was used for analysing the degree of dissimilarity  
439 between Rao's Q and Shannon H index across two high complex land cover  
440 types; i) montado, and ii) polyculture. To do so, a sample of 60 squares with  
441  $250 \times 250$  meters size was randomly selected over these two land cover types.  
442 Each square represents a sample of 625 S2A NDVI pixels, thus corresponding  
443 to a total of 37,500 pixels over the 60 squares. For the comparison between  
444 both indices, the coefficient of variation (CV) was calculated for each  $250 \times$   
445  $250$  m squares. Regarding the Rao's Q performance, Figure 6 clearly points  
446 to the significant improvements shown by Rao's Q index compared to the  
447 Shannon H index in describing the spatial diversity. In particular, it can be  
448 seen through the Figure 6, that Rao's Q index can highlight different gra-  
449 dients of spatial diversity of montado areas, which present high tree density  
450 variability (Figure 6), and thus high spatial heterogeneity. One-way ANOVA  
451 tests revealed that both indices values were significantly different between  
452 the two land cover types (montado:  $F = 503.3$ ,  $p < 0.001$ ; polyculture:  $F =$   
453  $889.8$ ,  $p < 0.001$ ). Overall, the obtained results demonstrate the capability of  
454 Rao's Q index in producing accurate landscape diversity maps in a complex  
455 landscape such as the Mediterranean agro-forestry systems.

## 456 7 Conclusion

457 In this paper, we showed several methods based on ecological  $\beta$ -diversity,  
458 which can be investigated by remote sensing through the calculation of  
459 ecosystem heterogeneity, to estimate the spatial variability of biodiversity.  
460 When there is a wide range of heterogeneity, for example when the data  
461 include homogeneous and heterogeneous zones, no single measure might cap-  
462 ture all the different aspects of  $\beta$ -diversity (e.g. Baselga (2013)). That is why  
463 we suggested in this manuscript multivariate and multidimensional methods  
464 (e.g. multivariate statistics and multidimensional distance matrices) based  
465 on the spectral signal and its variability over space to account for different  
466 aspects of diversity, also including distance- and abundance-based methods  
467 (e.g. the Rao's Q).

468 Biodiversity measured as species richness is often used for conservation  
469 purposes, hence the importance of avoiding an under- or over-estimate has

470 been highlighted (Chiarucci et al., 2009). Furthermore, pairwise distance-  
471 based methods might be profitably used to detect not only diversity hotspots  
472 in an area but also the variation of biodiversity over space, and potentially  
473 over time, once multitemporal sets of images are used.

474 In this paper we focused on optimising measures of  $\beta$ -diversity based on  
475 remote sensing data. Such measures might be used to regress species diversity  
476 against remotely sensed heterogeneity, based on new regression techniques  
477 which maximise the possibility of predicting the zones in a study area, or at  
478 larger spatial scales, of peculiar conservation value. As an example, shrink-  
479 age regression, recently applied in biodiversity conservation (Authier et al.,  
480 2017) could allow a direct focus on habitat modelling, which is one of the  
481 major strengths of remote sensing (Gillespie et al., 2008). Moreover, such  
482 analysis might be performed in a Bayesian framework allowing to i) model  
483 multidimensional covariates with non-stationary variation over space (Ran-  
484 dell et al., 2016), such as the bands of satellite images, and ii) model the  
485 errors in the output and their variation over space (Rocchini et al., 2017).

486 As previously stated, the suggested methods for  $\beta$ -diversity estimation  
487 from remote sensing are mainly based on distances, but they could be effec-  
488 tively translated to relative abundance-based methods. As an example Roc-  
489 chini et al. (2013) introduced the possibility of applying generalized entropy  
490 theory to satellite images with one single formula representing a continuum  
491 of diversity measures changing one parameter. One of the best examples  
492 in this framework could be the use of Hill numbers, in which diversity is  
493 expressed as:

$${}^qD = \left( \sum_{i=1}^S p_i^q \right)^{\frac{1}{1-q}} \quad (6)$$

494 where  $S$  = number of samples / pixels and  $p_i$  = relative abundance of a  
495 species / spectral value. varying the parameter  $q$ ,  ${}^qD$  varies accordingly in  
496 several diversity indices, e.g. for  $q = 0$   ${}^qD$  is the simple number of species,  
497 for  $\lim(q) = 1$   ${}^qD$  equals Shannon's entropy, etc. (Hsieh et al., 2016).

498 Furthermore, connectivity analysis might also be taken into account (Moila-  
499 nen et al., 2005, 2009). For instance, a remote sensing based connectivity  
500 network among different sites, based on  $\beta$ -diversity measures, could be ap-  
501 plied for the estimate of landscape connectivity and consequent genetic flow,  
502 as demonstrated by Vernesi et al. (2012). It has also been shown that commu-  
503 nity related biodiversity indicators are often missing from current monitoring  
504 programmes (Vihervaara et al., 2017); thus methods such as remote sensing  
505 based Rao's Q diversity applied for various ecosystems might improve other-  
506 wise challenging monitoring of biological communities.

507 With this manuscript we hope to stimulate discussion on the available  
508 methods for estimating  $\beta$ -diversity from remotely sensed imagery by propos-  
509 ing innovative techniques grounded on ecological theory.

## 510 Acknowledgments

511 We are grateful to the handling Editor and to two anonymous reviewers  
512 who improved with skillful suggestions a previous version of the present  
513 manuscript.

## 514 Authors' contribution statement

515 All authors contributed to the development and writing of the manuscript.

## 516 References

- 517 Alahuhta, J., Kosten, S., Akasaka, M., Auderset, D., Azzella, M., Bolpagni,  
518 R., Bove, C.P., Chambers, P.A., Chappuis, E., Ilg, C., Clayton, J., de  
519 Winston, M., Ecke, F., Gacia, E., Gecheva, G., Grillas, P., Hauxwell,  
520 J., Hellsten, H., Hjort, J., Hoyer, M.V., Kolada, K., Kuoppala, M., Lau-  
521 ridsen, T., Li, E.-H., Lukács, B.A., Mjelde, M., Mikulyuk, A., Mormul,  
522 R.P., Nishihiro, J., Oertli, B., Rhazi, L., Rhazi, M., Sass, L., Schranz, C.,  
523 Søndergaard, M., Yamanouchi, T., Yu, Q., Wang, H., Willby, N., Zhang,  
524 X.-K., Heino, J. (2017). Global variation in the beta diversity of lake  
525 macrophytes is driven by environmental heterogeneity rather than lati-  
526 tude. *Journal of Biogeography*, in press.
- 527 Asner, G., Martin, R., 2008. Spectral and chemical analysis of tropical forests:  
528 Scaling from leaf to canopy levels. *Remote Sens. Environ.* 112, 3958–3970.  
529 doi:10.1016/j.rse.2008.07.003
- 530 Asner, G.P., Martin, R.E., Anderson, C.B., Knapp, D.E., 2015. Quantifying  
531 forest canopy traits: Imaging spectroscopy versus field survey. *Remote*  
532 *Sens. Environ.* 158, 15–27. doi:10.1016/j.rse.2014.11.011
- 533 Authier, M., Saraux, C., Peron, C. (2017). Variable selection and accurate  
534 predictions in habitat modelling: a shrinkage approach. *Ecography*, 40:  
535 549-560.



- 536 Baselga, A. (2013). Multiple site dissimilarity quantifies compositional het-  
537 erogeneity among several sites, while average pairwise dissimilarity may be  
538 misleading. *Ecography*, 36: 124-128.
- 539 Baldeck, C., Asner, G., 2013. Estimating Vegetation Beta Diversity from Air-  
540 borne Imaging Spectroscopy and Unsupervised Clustering. *Remote Sens.*  
541 5, 2057–2071. doi:10.3390/rs5052057
- 542 Baldeck, C.A., Colgan, M.S., Féret, J.-B., Levick, S.R., Martin, R.E., Asner,  
543 G.P., 2014. Landscape-scale variation in plant community composition of  
544 an African savanna from airborne species mapping. *Ecol. Appl.* 24, 84–93.  
545 doi:10.1890/13-0307.1
- 546 Chadwick, K., Asner, G., 2016. Organismic-Scale Remote Sensing of  
547 Canopy Foliar Traits in Lowland Tropical Forests. *Remote Sens.* 8, 87.  
548 doi:10.3390/rs8020087
- 549 Chiarucci, A., Bacaro, G., Rocchini, D., Ricotta, C., Palmer, M.W., Scheiner,  
550 S.M. (2009). Spatially constrained rarefaction: incorporating the autocor-  
551 related structure of biological communities in sample-based rarefaction.  
552 *Community Ecology*, 10: 209-214.
- 553 Chon, T.-S., Park, Y.S., Moon, K.Y., Cha, E.Y. (1996). Patternizing com-  
554 munities by using an artificial neural network. *Ecological Modelling*, 90:  
555 69-78.
- 556 Clark, M., Roberts, D., Clark, D., 2005. Hyperspectral discrimination of trop-  
557 ical rain forest tree species at leaf to crown scales. *Remote Sens. Environ.*  
558 96, 375–398. doi:10.1016/j.rse.2005.03.009
- 559 Clark, M.L., Roberts, D.A., 2012. Species-Level Differences in Hyperspectral  
560 Metrics among Tropical Rainforest Trees as Determined by a Tree-Based  
561 Classifier. *Remote Sens.* 4, 1820–1855. doi:10.3390/rs4061820
- 562 Feilhauer, H., Faude, U., Schmidtlein, S., 2011. Combining Isomap ordina-  
563 tion and imaging spectroscopy to map continuous floristic gradients in a  
564 heterogeneous landscape. *Remote Sens. Environ.* 115, 2513–2524.
- 565 Feilhauer, H., Doktor, D., Lausch, A., Schmidtlein, S., Schulz, G., Stenzel,  
566 S., 2014. Mapping Natura 2000 habitats and their local variability with  
567 remote sensing. *Appl. Veg. Sci.* 17, 765–779.
- 568 Feilhauer, H., Doktor, D., Schmidtlein, S., Skidmore, A.K., 2016. Mapping  
569 pollination types with remote sensing. *J. Veg. Sci.* 27, 999-1011.

- 570 Feilhauer, H., Schmidtlein, S., 2009. Mapping continuous fields of alpha and  
571 beta diversity. *Appl. Veg. Sci.* 12, 429–439.
- 572 Feilhauer, H., Thonfeld, F., Faude, U., et al., 2013. Assessing floristic com-  
573 position with multispectral sensors a comparison based on monotempo-  
574 ral and multiseasonal field spectra. *Int. J. Appl. Earth Obs. Geoinf.* 21,  
575 218–229.
- 576 Féret, J.-B., Asner, G.P., 2014a. Mapping tropical forest canopy diver-  
577 sity using high-fidelity imaging spectroscopy. *Ecol. Appl.* 24, 1289–1296.  
578 doi:10.1890/13-1824.1
- 579 Féret, J.-B., Asner, G.P., 2014b. Microtopographic controls on lowland  
580 Amazonian canopy diversity from imaging spectroscopy. *Ecol. Appl.* 24,  
581 1297–1310. doi:10.1890/13-1896.1
- 582 Féret, J.-B., Asner, G.P., 2013. Tree Species Discrimination in Tropical  
583 Forests Using Airborne Imaging Spectroscopy. *IEEE Trans. Geosci. Re-  
584 mote Sens.* 51, 73–84. doi:10.1109/TGRS.2012.2199323
- 585 Ferrier, S., Manion, G., Elith, J., Richardson, K. (2007) Using generalized  
586 dissimilarity modelling to analyse and predict patterns of beta diversity in  
587 regional biodiversity assessment. *Diversity and Distributions*, 13, 252-264.
- 588 Foody, G.M. (1999). Applications of the self-organising feature map neural  
589 network in community data analysis. *Ecological Modelling*, 120: 97-107.
- 590 Foody, G.M., Cutler, M.E.J. (2003). Tree biodiversity in protected and logged  
591 Bornean tropical rain forests and its measurement by satellite remote sens-  
592 ing. *Journal of Biogeography*, 30: 1053-1066.
- 593 Fritzke, B., 1995. Growing grid-a self organizing network with constant neigh-  
594 borhood range and adaptation strength. *Neural Processing Letters*, 2: 9-  
595 13.
- 596 Giraudel, J.L., Lek, S. (2001). A comparison of SOM algorithm and some con-  
597 ventional statistical methods for ecological community ordination. *Ecolog-  
598 ical Modelling*, 146: 329-339.
- 599 Godinho, S., Gil, A., Guiomar, N., Neves, N. and Pinto-Correia, T. 2016.  
600 A remote sensing-based approach to estimating montado canopy density  
601 using the FCD model: a contribution to identifying HNV farmlands in  
602 southern Portugal. *Agroforestry Systems* 90:23-34.

- 603 Gillespie, T.W. (2005). Predicting woody-plant species richness in tropical  
604 dry forests: a case study from South Florida, U.S.A. *Ecological Applica-*  
605 *tions*, 15: 27-37.
- 606 Gillespie, T.W., Foody, G.M., Rocchini, D., Giorgi, A.P., Saatchi, S. (2008).  
607 Measuring and modeling biodiversity from space. *Progress in Physical Geo-*  
608 *graphy*, 32: 203-221.
- 609 Graham, C.H., Fine, P.V.A. (2008) Phylogenetic beta diversity: linking eco-  
610 logical and evolutionary processes across space in time. *Ecology Letters*,  
611 11, 1265-1277
- 612 Gu, H., Singh, A., Townsend, P.A., 2015. Detection of gradients of forest  
613 composition in an urban area using imaging spectroscopy. *Remote Sens.*  
614 *Environ.* 167, 168-180.
- 615 Harris, A., Charnock, R., Lucas, R.M., 2015. Hyperspectral remote sensing  
616 of peatland floristic gradients. *Remote Sens. Environ.* 162, 99–111.
- 617 Heino, J., Melo, A.S., Bini, L.M., Altermatt, F., Al-Shami, S.A, Angeler, D.,  
618 Bonada, N., Brand, C., Callisto, M., Cottenie, K., Dangles, O., Dudgeon,  
619 D., Encalada, A., Göthe, E., Grönroos, M., Hamada, N., Jacobsen, D.,  
620 Landeiro, V.L., Ligeiro, R., Martins, R.T., Miserendino, M. L., Md Rawi,  
621 C.S. Rodrigues, M., Roque, F.O., Sandin, L., Schmera, D., Sgarbi, L.F.,  
622 Simaika, J., Siqueira, T., Thompson, R.M., Townsend, C.R. (2015) A  
623 comparative analysis reveals weak relationships between ecological factors  
624 and beta diversity of stream insect metacommunities at two spatial levels.  
625 *Ecology and Evolution* 5, 1235-1248.
- 626 Hsieh, T.C., Ma, K.H., Chao, A. (2016). iNEXT: an R package for rarefaction  
627 and extrapolation of species diversity (Hill numbers). *Methods in Ecology*  
628 *& Evolution* 2016, 7: 1451-1456.
- 629 Hernandez-Stefanoni, J.L., Gallardo-Cruz, J.A., Meave, J.A., Rocchini, D.,  
630 Bello-Pineda, J., López-Martínez, J.O., 2012. Modeling  $\alpha$ - and  $\beta$ -diversity  
631 in a tropical forest from remotely sensed and spatial data. *Int. J. Appl.*  
632 *Earth Observ. Geoinform.* 19, 359-368.
- 633 Hill, M.O., Gauch, H.G., 1980. Detrended correspondence analysis: an im-  
634 proved ordination technique. *Vegetatio* 42, 47–58.
- 635 Kohonen, T. (1982). Analysis of a simple self-organizing process. *Biological*  
636 *Cybernetics*, 44: 135-140.

- 637 Latombe, G., Hui, C., McGeoch, M.A. (2017) Multi-site generalised dissimi-  
638 larity modelling: using zeta diversity to differentiate drivers of turnover in  
639 rare and widespread species. *Methods in Ecology and Evolution*, 8, 431-  
640 442.
- 641 Lausch, A., Bannehr, L., Beckmann, M., Boehm, C., Feilhauer, H., Hacker,  
642 J.M., Heurich, M., Jung, A., Klenke, R., Neumann, C., Pause, M., Roc-  
643 chini, D., Schaepman, M.E., Schmidlein, S., Schulz, K., Selsam, P., Set-  
644 tele, J., Skidmore, A.K., Cord, A.F. (2016). Linking Earth Observation  
645 and taxonomic, structural and functional biodiversity: Local to ecosystem  
646 perspectives. *Ecological Indicators*, 70: 317-339.
- 647 Leathwick, J.R., Snelder, T., Chadderton, W.L., Elith, J., Julian, K., Ferrier,  
648 S. (2011). Use of generalised dissimilarity modelling to improve the biolog-  
649 ical discrimination of river and stream classifications. *Freshwater Biology*,  
650 56, 21-38.
- 651 Legendre, P., Borcard, D., Peres-Neto, P.R. (2005) Analyzing beta diver-  
652 sity: Partitioning the spatial variation of community composition data.  
653 *Ecological Monographs*, 75, 435-450.
- 654 Leitão, P.J., Schwieder, M., Suess, S., Catry, I., Milton, E.J., Moreira, F.,  
655 Osborne, P.E., Pinto, M.J., van der Linden, S., Hostert, P. (2015) Map-  
656 ping beta diversity from space: sparse generalised dissimilarity modelling  
657 (SGDM) for analysing high-dimensional data. *Methods in Ecology and*  
658 *Evolution*, 6, 764-771.
- 659 Leitão, P., Schwieder, M., Senf, C. (2017) *sgdm*: An R Package for Perform-  
660 ing Sparse Generalized Dissimilarity Modelling with Tools for *gdm*. *ISPRS*  
661 *International Journal of Geo-Information*, 6, 23.
- 662 Mantel, N., Valand, R.S. (1970) A technique of nonparametric multivariate  
663 analysis. *Biometrics*, 26, 547-558.
- 664 Mazor, T., Kark, S., Possingham, H.P., Rocchini, D., Levy, Y., Richardson,  
665 A.J., Levin, N. (2013). Can satellite-based night lights be used for conser-  
666 vation? The case of nesting sea turtles in the Mediterranean. *Biological*  
667 *Conservation*, 159: 63-72.
- 668 Meentemeyer, R.K., Anacker, B.L., Mark, W., Rizzo, D.M. (2008). Early  
669 detection of emerging forest disease using dispersal stimation and ecological  
670 niche modeling. *Ecological Applications*, 18: 377-390.

- 671 Metz, M., Rocchini, D., Neteler, M. (2014). Surface temperatures at the  
672 continental scale: tracking changes with remote sensing at unprecedented  
673 detail. *Remote Sensing*, 6: 3822-3840.
- 674 Moilanen, A., Franco, A.M.A., Early, R., Fox, R., Wintle, B., Thomas, C.D.  
675 (2005). Prioritizing multiple-use landscapes for conservation: methods for  
676 large multi-species planning problems. *Proceedings of the Royal Society B:  
677 Biological Sciences*, 272: 1885-1891.
- 678 Moilanen, A., Kujala, H., Leathwick, J.R. (2009). The zonation framework  
679 and software for conservation prioritization. in A. Moilanen, K. Wilson,  
680 H.P. Possingham (Eds.), *Spatial Conservation Prioritization: Quantitative  
681 Methods Computational Tools*, Oxford University Press (2009), pp. 196-  
682 210.
- 683 Neumann, C., Weiss, G., Schmidlein, S., Itzerott, S., Lausch, A., Doktor,  
684 D., Brell, M., 2015. Ecological gradient-based habitat quality assessment  
685 for spectralecosystem monitoring. *Remote Sens.* 7, 2871–2898.
- 686 Palmer, M.W., Earls, P.G., Hoagland, B.W., White, P.S., Wohlgemuth, T.,  
687 2002. Quantitative tools for perfecting species lists. *Environmetrics* 13,  
688 121–137. doi:10.1002/env.516
- 689 QGIS Development Team, 2016. QGIS Geographic Information System.  
690 Open Source Geospatial Foundation. <http://qgis.osgeo.org>
- 691 Randell, D., Turnbull, K., Ewans, K., Jonathan, P. (2016). Bayesian inference  
692 for nonstationary marginal extremes. *Environmetrics*, 27: 439-450.
- 693 Rocchini, D. (2007). Distance decay in spectral space in analysing ecosystem  
694  $\beta$ -diversity. *International Journal of Remote Sensing*, 28: 2635-2644.
- 695 Rocchini, D., Andreini Butini, S., Chiarucci, A. (2005). Maximizing plant  
696 species inventory efficiency by means of remotely sensed spectral distances.  
697 *Global Ecology and Biogeography*, 14: 431-437.
- 698 Rocchini, D., Balkenhol, N., Carter, G.A., Foody, G.M. Gillespie, T.W., He,  
699 K.S., Kark, S., Levin, N., Lucas, K., Luoto, M., Nagendra, H., Oldeland,  
700 J., Ricotta, C., Southworth, J., Neteler, M. (2010). Remotely sensed spec-  
701 tral heterogeneity as a proxy of species diversity: recent advances and open  
702 challenges. *Ecological Informatics*, 5: 318-329.
- 703 Rocchini, D., Boyd, D.S., Féret, J.B., Foody, G.M., He, K.S., Lausch, A.,  
704 Nagendra, H., Wegmann, M., Pettorelli, N. (2016). Satellite remote sensing

- 705 to monitor species diversity: potential and pitfalls. *Remote Sensing in*  
706 *Ecology and Conservation*, 2: 25-36.
- 707 Rocchini, D., Delucchi, L., Bacaro, G., Cavallini, P., Feilhauer, H., Foody,  
708 G.M., He, K.S., Nagendra, H., Porta, C., Ricotta, C., Schmidtlein, S.,  
709 Spano, L.D., Wegmann, M., Neteler, M. (2013). Calculating landscape  
710 diversity with information-theory based indices: A GRASS GIS solution.  
711 *Ecological Informatics*, 17: 82-93.
- 712 Rocchini, D., Garzon-Lopez, C.X., Marcantonio, M., Amici, V., Bacaro, G.,  
713 Bastin, L., Brummitt, N., Chiarucci, A., Foody, G.M., Hauffe, H.C., He,  
714 K.S., Ricotta, C., Rizzoli, A., Rosá, R. (2017). Anticipating species dis-  
715 tributions: handling sampling effort bias under a Bayesian framework.  
716 *Science of the Total Environment*, 584-585, 282-290.
- 717 Rocchini, D., Hernández Stefanoni, J.L., He, K.S: (2015). Advancing species  
718 diversity estimate by remotely sensed proxies: a conceptual review. *Eco-*  
719 *logical Informatics*, 25: 22-28.
- 720 Rocchini, D., Neteler, M. (2012). Let the four freedoms paradigm apply to  
721 ecology. *Trends in Ecology & Evolution*, 27: 310–311.
- 722 Rosauer, D.F., Ferrier, S., Williams, K.J., Manion, G., Keogh, J.S., Laffan,  
723 S.W. (2014) Phylogenetic generalised dissimilarity modelling: a new ap-  
724 proach to analysing and predicting spatial turnover in the phylogenetic  
725 composition of communities. *Ecography*, 37, 21-32.
- 726 Schmidtlein, S., Sassin, J., 2004. Mapping continuous floristic gradients  
727 in grasslands using hyperspectral imagery. *Remote Sens. Environ.* 92,  
728 126–138.
- 729 Schmidtlein, S., Zimmermann, P., Schüpferling, R., Weiss, C., 2007. Mapping  
730 the floristic continuum: ordination space position estimated from imaging  
731 spectroscopy. *Journal of Vegetation Science*, 18: 131–140.
- 732 Tuomisto, H., Poulsen, A., Ruokolainen, K., Moran, R., Quintana, C., Celi,  
733 J., Canas, G. (2003). Linking floristic patterns with soil heterogeneity and  
734 satellite imagery in Ecuadorian Amazonia. *Ecological Applications*, 13:  
735 352-371.
- 736 Tuomisto, H., Ruokolainen, K., 2006. Analyzing or explaining beta diversity?  
737 Understanding the targets of different methods of analysis. *Ecology* 87,  
738 2697–2708. doi:10.1890/0012-9658(2006)87[2697:AOEBDU]2.0.CO;2

- 739 Tyre, A.J., Possingham, H.P., Lindenmayer, D.B. (2001). Inferring process  
740 from pattern: can territory occupancy provide information about life his-  
741 tory parameters? *Ecological Applications*, 11: 1722-1737.
- 742 Tahvanainen, T. (2011). Abrupt ombrotrophication of a boreal aapa mire  
743 triggered by hydrological disturbance in the catchment. *Journal of Ecology*  
744 2011, 99: 404-415.
- 745 Ustin, S.L., Gamon, J.A., 2010. Remote sensing of plant functional types.  
746 *New Phytol.* 186, 795–816.
- 747 Vaglio Laurin, G., Chan, J.C.-W., Chen, Q., Lindsell, J.A., Coomes, D.A.,  
748 Guerriero, L., Frate, F.D., Miglietta, F., Valentini, R., 2014. Biodiversity  
749 Mapping in a Tropical West African Forest with Airborne Hyperspectral  
750 Data. *PLoS ONE* 9, e97910. doi:10.1371/journal.pone.0097910
- 751 Vernesi, C., Rocchini, D., Pecchioli, E., Neteler, M., Vendramin, G.G., Paf-  
752 fetti, D. (2012). A landscape genetics approach reveals ecological-based  
753 differentiation in populations of holm oak (*Quercus ilex*, L.) at their north-  
754 ernmost distribution edge. *Biological Journal of the Linnean Society*, 107:  
755 458-467.
- 756 Vihervaara, P., Auvinen, A.-P, Mononen, L., Törmä, M., Ahlroth, P.,  
757 Anttila, S., Böttcher, K., Forsius, M., Heino, J., Heliölä, J., Koskelainen,  
758 M., Kuussaari, M., Meissner, K., Ojala, O., Tuominen, S., Viitasalo, M.,  
759 Virkkala, R. 2017: How Essential Biodiversity Variables and remote sens-  
760 ing can help national biodiversity monitoring. *Global Ecology and Conser-  
761 vation* 10: 43-59.
- 762 Wegmann, M. Leutner, B.F., Metz, M., Neteler, M., Dech, S., Rocchini,  
763 D. (2017). r.pi: a GRASS GIS package for semi-automatic spatial pat-  
764 tern analysis of remotely sensed land cover data. *Methods in Ecology and  
765 Evolution*.
- 766 Whittaker, R.H. (1960) Vegetation of the Siskiyou Mountains, Oregon and  
767 California. *Ecological Monographs*, 30, 280-338.
- 768 Witten, D., Tibshirani, R., Gross, S., Narasimhan, B. (2013) PMA: Penalized  
769 Multivariate Analysis.
- 770 Woolley, S.N.C., Foster, S.D., O'Hara, T.D., Wintle, B.A., Dunstan, P.K.  
771 (2017) Characterising uncertainty in generalised dissimilarity models.  
772 *Methods in Ecology and Evolution*, 8, 985-995.
- 773 Figures



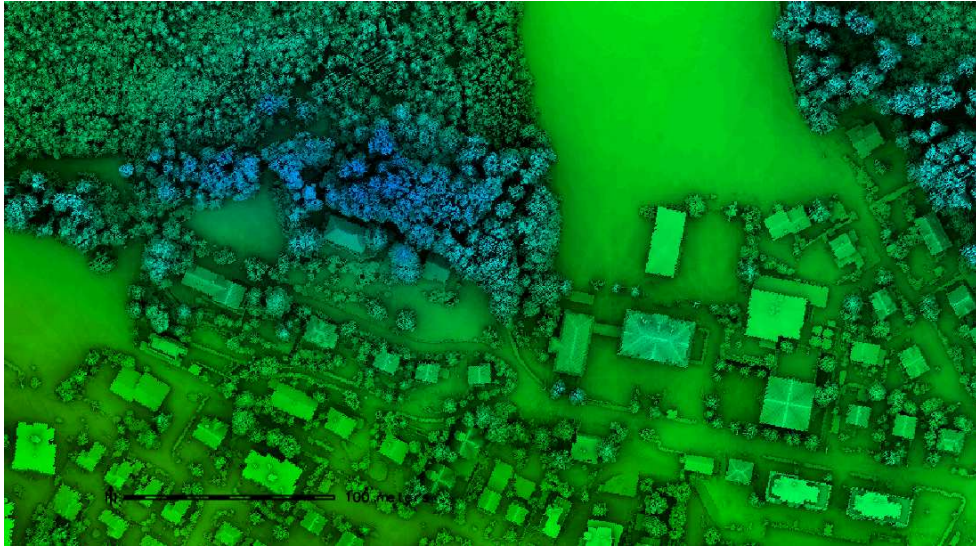


Figure 1: An example of how to couple information on compositional properties of the landscape by optical data together with structural (3D) properties by laser scanning LiDAR data.

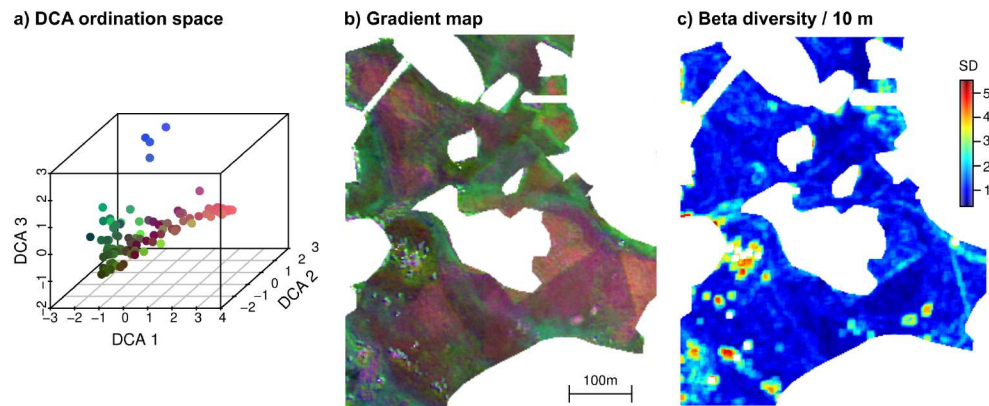


Figure 2:  $\beta$ -diversity assessment with a combination of ordination techniques and remote sensing. a) Three dimensional DCA ordination space of  $n=100$  vegetation plots sampled in raised bogs, fens, transition mires and *Molinia* meadows in the alpine foothills of Southern Germany. An inter-plot distance of 4 SD corresponds to a full species turnover. b) Maps of the ordination axes resulting from a spatial prediction based on canopy reflectance. Each pixel has a predicted position in the ordination space that is indicated by its color. The color scheme corresponds to a). The map has a spatial resolution of 2 m x 2 m, which is in line with the sampled plot size. c) Cumulative change rates along the three DCA axes in a 5 x 5 pixel neighborhood. A high change rate indicates a high beta diversity.

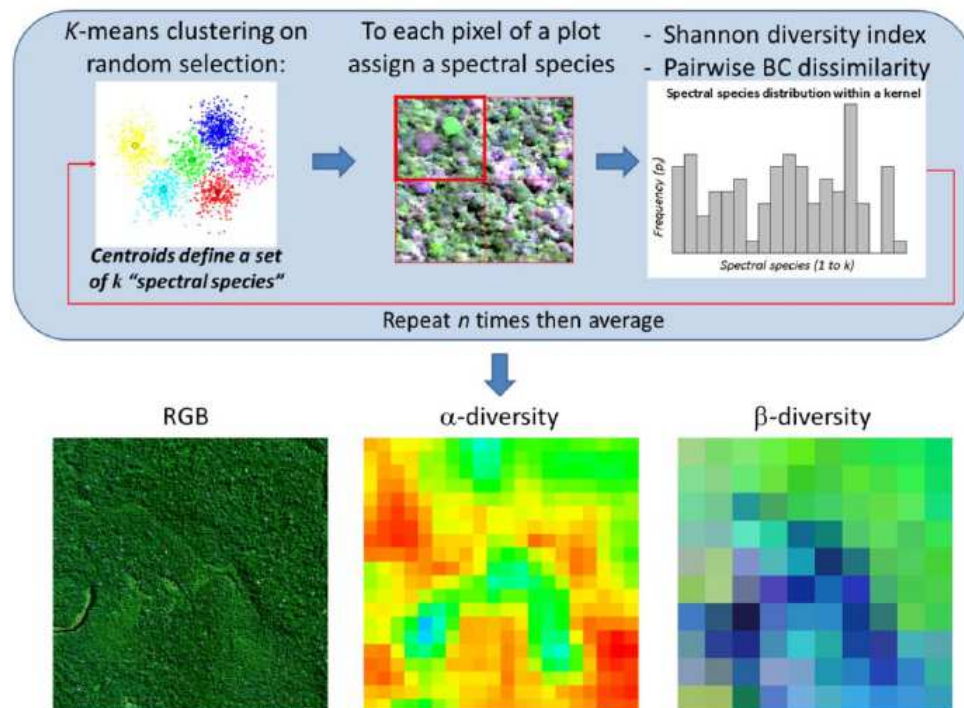


Figure 3: Spectral species can be identified in a hyper- or multi-spectral image by spatial clustering method and their distribution can be mapped. Such maps can further be used to apply local-based heterogeneity measurements ( $\alpha$ -diversity) as well as iterative distance based methods to build  $\beta$ -diversity maps. Reproduced from Féret and Asner (2014a).

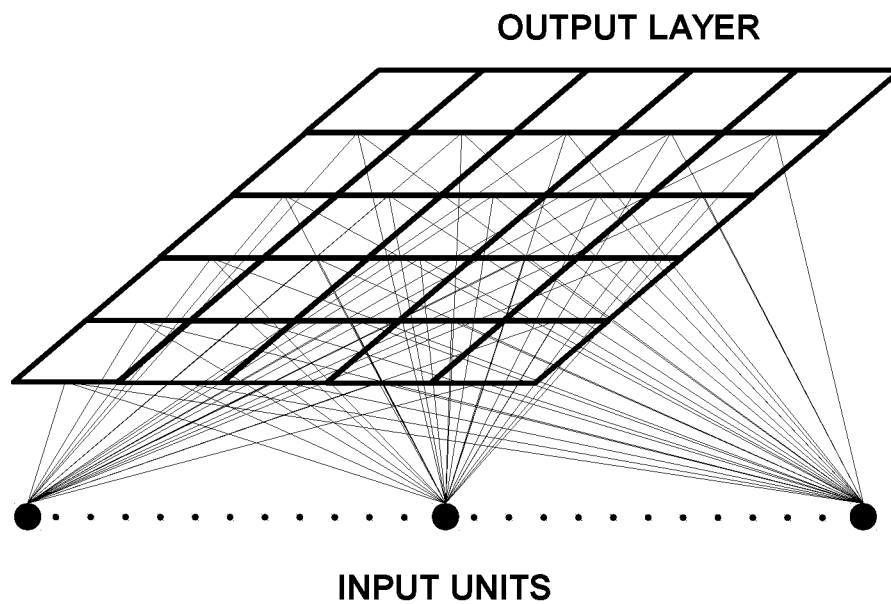


Figure 4: A self-organising feature map can be built starting from an input layer, e.g. the presence absence of a tree species or of a peculiar spectral value) which is connected to every unit in the output layer by a weighted connection. The self organising feature map uses unsupervised learning to map the location of field sites within the output space on the basis of their relative similarity in species or spectral composition. [Redrawn](#) from Foody and Cutler (2003).

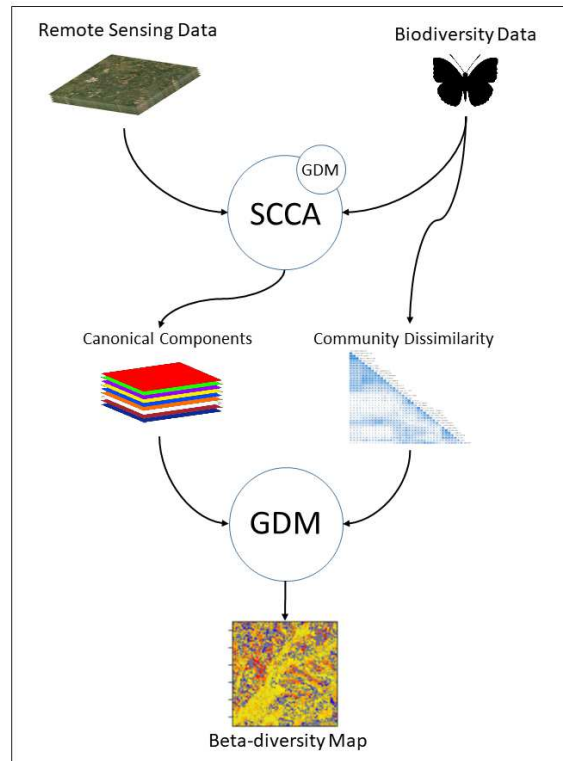


Figure 5: An example of the Sparse Generalized Dissimilarity Model (SGDM) approach. Remote sensing data and biodiversity data in the field can be coupled by Sparse Canonical Correlation Analysis to produce canonical components and a community dissimilarity matrix, which are then used to build a Generalized Dissimilarity Model to finally derived a  $\beta$ -diversity map.

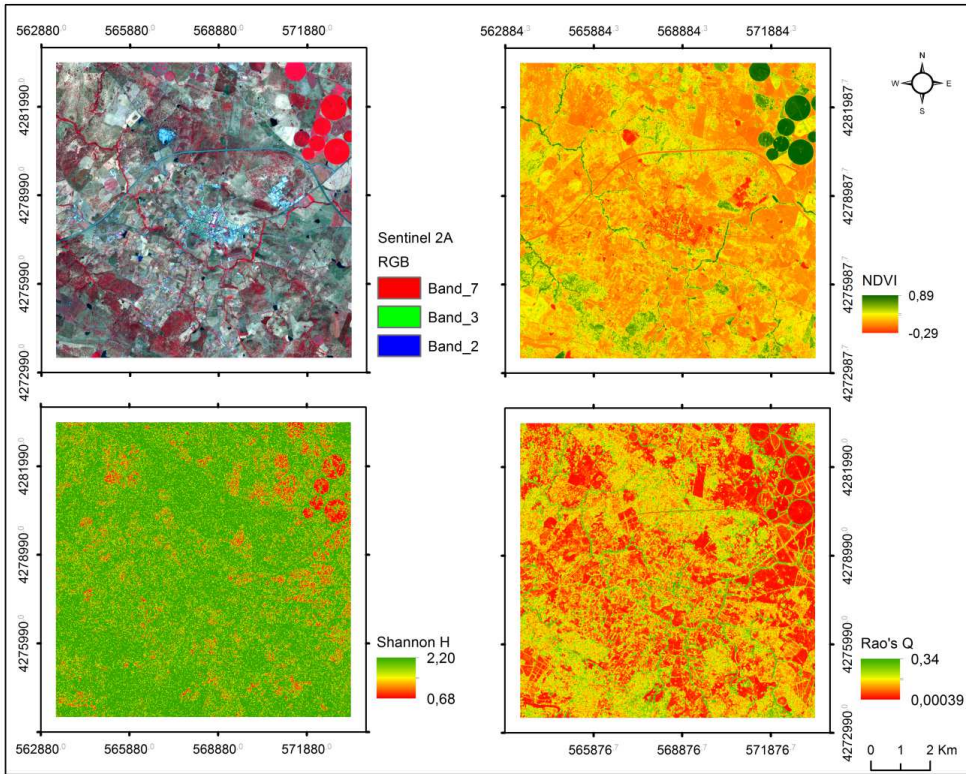


Figure 6: Upper panels: Sentinel-2A scene (8 August 2016) and derived NDVI for the agro-forestry systems test site located in southern Portugal. Lower panels: results from Shannon's H and Rao's Q indices computation. Shannon index tends to overestimate the landscape diversity when compared to the Rao's Q index.